

**FINAL REPORT
SEISMIC SURVEYS FOR INVESTIGATION OF SUBSURFACE FAULTING
AT NORTH HAIWEE DAM INYO COUNTY, CALIFORNIA**



**December 13, 2012
ADVANCED GEOSCIENCE, INC.**

ADVANCED GEOSCIENCE, INC.

Geology and Geophysics
Subsurface Exploration

Non-Destructive Evaluation



24701 Crenshaw Blvd.
Torrance, California
90505 USA
Telephone (310) 378-7480
Fax (310) 872-5323
www.AdvancedGeoscience.com

December 13, 2012

Mr. Andrew Stanton, P.E.
Project Manager
Black & Veatch Corporation
800 Wilshire Boulevard
Suite 600
Los Angeles, California 90017

Re: **Final Report**
Seismic Surveys for Investigation of Subsurface Faulting
At North Haiwee Dam
Inyo County, California

Dear Mr. Stanton:

In accordance with our consulting agreement dated August 6, 2010 and its amendments, Advanced Geoscience presents this final report summarizing our field procedures, and methods of data processing and evaluation for the Phase 3 and 4 seismic surveys. This report also presents our final revised interpretation and mapping of the trend of subsurface faulting based on the seismic profiles from the Phase 1 through 4 surveys completed to date.

We trust this report meets your current needs. Please contact the undersigned for any additional discussion of these results.

Sincerely,
Advanced Geoscience, Inc.



Mark G. Olson, P.Gp., P.G., C.H.G.
Principal Geophysicist and Geologist

Table of Contents

1.0 INTRODUCTION	Page 1
2.0 SURVEY PROCEDURES	Page 2
2.1 PHASE 3- SEISMIC REFLECTION AND REFRACTION PROFILING ON LINES 6, 7, AND 8	Page 2
2.1.1 Data Collection	Page 3
2.1.2 Data Processing	Page 4
2.2 PHASE 4- SEISMIC REFLECTION AND REFRACTION PROFILING ON LINES 9, 10, AND 11	Page 6
2.2.1 Data Collection	Page 6
2.2.2 Data Processing	Page 8
3.0 DISCUSSION OF RESULTS	Page 9
3.1 GEOLOGIC INTERPRETATION OF SEISMIC PROFILES AND EVALUATION OF SUBSURFACE FAULTING	Page 9
3.1.1 Phases 1 and 2	Page 9
3.1.2 Phases 3 and 4	Page 12
3.2 MAPPING OF TREND OF SUBSURFACE FAULTING	Page 14
3.3 EVALUATION OF FAULT PLANE DETECTION LIMIT	Page 14
4.0 REFERENCES	Page 15
APPENDIX A	Page 16

List of Figures

- Figure 1- Site Map Showing Locations of Seismic Survey Lines and Interpretation of Subsurface Faulting
- Figure 2- Line 1 Seismic Reflection Profile
- Figure 3- Line 2 Seismic Reflection Profile
- Figure 4- Line 3 Seismic Reflection and Refraction Profiles
- Figure 5- Line 4 Seismic Reflection and Refraction Profiles
- Figure 6- Line 5 Seismic Reflection and Refraction Profiles
- Figure 7- Line 6 Seismic Reflection and Refraction Profiles
- Figure 8- Line 7 Seismic Reflection and Refraction Profiles
- Figure 9- Line 8 Seismic Reflection and Refraction Profiles
- Figure 10- Line 9 Seismic Reflection and Refraction Profiles
- Figure 11- Line 10 Seismic Reflection and Refraction Profiles
- Figure 12- Line 11 Seismic Reflection and Refraction Profiles
- Figure 13- Line 9 Seismic Reflection Profile of East Abutment Area Showings Correlation to Sonic Borehole Logs

1.0 INTRODUCTION

This report summarizes the results of the seismic surveys completed to date at the North Haiwee Dam by Advanced Geoscience, Inc. These surveys were conducted in four separate phases of field operations, referred to as “Phases 1 through 4”. Phases 1 and 2 were performed in December, 2008 and March, 2009. Phases 3 and 4 were performed in February, 2011 and June, 2012. The data from each of these field surveys were used to prepare seismic reflection and refraction profiles showing images of subsurface geologic layering. These seismic profile images were used to interpret structural and stratigraphic conditions to investigate faulting.

The Phase 1 and 2 seismic surveys were initiated as a result of the geologic investigation completed by URS Corporation in December, 2007. This investigation discovered conditionally active faulting in trenches on the eastern margin of the North Haiwee reservoir about 0.5 miles south of the existing dam. The seismic surveys were used to investigate whether this faulting (identified by URS as “Fault A”) could extend northward to the footprint of the existing dam and the proposed replacement dam shown on the site map in Figure 1.

The Phase 1 and 2 seismic surveys were setup to first provide a multi-scale investigation of subsurface faulting. In Phase 1, seismic data were first recorded along two 7,300-foot long survey lines designated as Lines 1 and 2 (Figure 1). These data were recorded with a vibroseis seismic energy source to prepare deeper reflection profiles across the area to investigate basin structure and faulting to depths exceeding 3,000 feet. In Phase 2, higher-resolution, near-surface seismic reflection and refraction data were recorded along three, shorter-length, 850 to 1,250-foot long survey lines designated as Lines 3, 4, and 5 (Figure 1). These higher-resolution surveys were recorded with a shotgun shell energy source to investigate faulting in the upper 600 to 800 feet below the ground surface. The initial interpretation of faulting from Lines 1 and 2 (in Phase 1) was used to position Lines 3 and 4 to investigate areas where there was evidence of deeper fault planes projecting upward near the surface. Line 5 was positioned further to the south on the eastside of the reservoir near Trenches T-3e and T-3f where URS discovered Fault A. All of the survey lines were positioned along southwest-to-northeast traverses to cross the possible northwest-to-north trend of Fault A.

The results of this previous investigation are discussed in our report to the Los Angeles Department of Water and Power titled: “Phase 1 and 2 Seismic Surveys for Investigation of Subsurface Faulting at North Haiwee Dam Inyo County, California”, dated September 7, 2009. This earlier report provided an initial interpretation of subsurface faulting based on the seismic profiles for Lines 1 through 5. This interpretation first identified two patterns of faulting which were labeled as “A1 through A3” and “C1 through C3”. The site map in this earlier report provided an initial mapping of the trend of this faulting. The seismic profiles for Lines 1 through 5 are re-displayed in this report in Figures 2 through 6 with our revised interpretation of this faulting.

The Phase 3 surveys were initiated based on results of the Phase 1 and 2 seismic surveys. Additional seismic reflection and refraction data were recorded along three southwest-to-northeast survey lines designated as Lines 6, 7, and 8 to help confirm or revise the initial interpretation of subsurface faulting and more accurately map its trend. The data were recorded using procedures similar to the procedures used for Lines 3 and 4 in Phase 2. The positions of these survey lines are shown on the site map in Figure 1. Lines 7 and 8 were positioned from the west side of the river valley to the elevated terrace area east of the valley to investigate the subsurface on each side of the proposed replacement dam and the possibility of a right-stepping, eastward shift in the trends of the A1-A3 and C1-C3 faults. Line 6 was positioned southeast of the dam to investigate the connection of the faults interpreted on the seismic profiles to Fault A. The profiles for Lines 6, 7, and 8 are shown in Figures 7 through 9.

The Phase 4 surveys were initiated based on results of the Phase 3 surveys. Seismic reflection and refraction data were recorded along Lines 9, 10, and 11 (Figure 1) to provide better imaging of alluvial interfaces and bedding in the upper part of the Coso Formation. Line 9 was positioned along the axis of the proposed replacement dam and extended to the east to provide subsurface coverage across the right abutment of the dam and the elevated terrace area. This line was used to investigate the C1-C2 and A1 faults near the proposed dam, and help confirm the interpretation that no younger faulting exists beneath the dam's axis in the valley. Line 10 was positioned along a northwest-to-southeast orientation to better correlate the R1-R3 reflection patterns across Lines 1, 6, 9, and 8. Line 11 was positioned in the canyon area north of Line 5 on the east side of the reservoir, extending from the shoreline to the BLM property line. Line 11 was positioned to provide a better mapping of the A1-A4 fault planes between Lines 5 and 6 and the connection of this faulting to Fault A.

The section below summarizes the Phase 3 and 4 seismic data collection and data processing procedures. The concluding section discusses our geologic interpretation of all the seismic profiles and our current, revised evaluation of subsurface faulting. This section also presents our revised mapping of the trend of this faulting.

2.0 SURVEY PROCEDURES

2.1 PHASE 3- SEISMIC REFLECTION AND REFRACTION PROFILING ON LINES 6, 7 AND 8

The seismic surveys along Lines 6, 7 and 8 were conducted from February 8 through 26, 2011. Lines 7 and 8 were recorded first and positioned from the west side of the valley to the elevated terrace area east of the valley. These lines were positioned to investigate the subsurface north and south of the proposed replacement dam, and the possibility of a right-stepping, eastward shift in the trends of the faults interpreted in Phase 1 and 2. Line 6 was positioned southeast of the existing dam to investigate the connection of the faults interpreted in Phase 1 and 2 to Fault A.

During these field surveys our crew experienced periods of adverse weather

conditions consisting mostly of high winds. This resulted in some delays in the seismic data recording, and the need to improvise in the field a higher-output seismic energy source.

2.1.1 Data Collection

Advanced Geoscience's survey crew first setup stakes at 100-foot intervals along each of the survey lines to establish geophone stationing. These control points primarily followed the flagged traverses for Lines 6 through 8 positioned earlier by LADWP. However, some slight deviations were made to position the lines away from areas later identified by the biologist and archeologist field monitors. After the seismic surveys were completed LADWP land surveyors measured the coordinates and elevations of these control points. These location measurements were later provided to us in a computer spreadsheet file.

The field procedures were setup to record one seismic data set for each of the three survey lines. These data sets consisted of "field records" which were used to generate separate seismic reflection and refraction profiles along Lines 6, 7, and 8.

A Seistronix 132-channel, EX-6 seismic data recording system was used to record the seismic data. The EX-6 system was connected to 126-channel, geophone receiver arrays (or "spreads") setup along each survey line. Each survey line consisted of multiple, overlapping geophone spreads with 126 40-Hertz geophones spaced 10-feet apart. The following lists the total length of geophone coverage setup along the survey lines:

Line 6	1,490 feet
Line 7	3,650 feet
Line 8	4,190 feet

Seismic waves were transmitted into the ground at "shot points" positioned along the survey lines and recorded into the 126-channel geophone spreads moved along the line. The energy source for these seismic waves was generated by firing multiple 400-grain shotgun shell blanks beneath the ground in shallow auger borings 2 to 3 feet deep. At each shot point location shotgun shell blanks were bundled together and electrically fired to release a single impulsive seismic energy source into the ground. Due to higher levels of background noise from strong wind gusts a greater number of shotgun shell blanks had to be used to improvise a higher output seismic energy source. At many of the shot point locations 5 shotgun shell blanks were bundled together and used to increase this energy output. All of the electrically-detonated shotgun shell blanks were purchased from Betsy Seisgun in Tulsa, Oklahoma.

The combined reflection and refraction data sets were recorded in a west-to-east movement along the survey lines. A 4WD Polaris Ranger was used to move the auger drill, seismic cables, geophones, and recording electronics along the survey lines. The central recording computer was setup inside a 4WD passenger vehicle which was also

moved along the survey lines.

Lines 6, 7, and 8 were recorded mostly with patterns of shot points positioned at 10-foot intervals along the survey lines. For Lines 6 and 8, the first shot point started 5-foot west of the first geophone position and continued along the line between each geophone position. For Line 7, the first shot point started at geophone station 205 feet and continued along the line between each geophone position. Line 8 was recorded first and followed by the recording of Line 7. Line 6 was recorded last. Due to the limited number of shotgun shell blanks available to complete Line 6 the last 700 feet of shot points along Line 6 were spaced at 10 and 20-foot intervals.

As the shot points moved to the east, the 126-channel geophone spreads were also shifted to the east in increments of 240-feet. This shift in geophone spread positioning was made after the shot points moved 120-feet past the centerline of each geophone spread. This “walk through” 126-channel geophone recording configuration was used to generate reflection datasets along Lines 6, 7, and 8 with maximum 80 to 90-fold subsurface coverage with 5-foot common-midpoint (CMP) reflection spacing.

The resulting surveys recorded a total of 113 field records for Line 6, 319 field records for Line 7, and 391 field records for Line 8. Each 126-channel field record was recorded with an 800 millisecond record length and 0.25 millisecond sampling rate with 24 bit analog-to-digital resolution.

The data quality of these field records was not quite as good as the Phase 2 survey’s field records. The Phase 3 field records showed random noise interference from stronger wind gusts and the frequency and phase characteristics of the reflection patterns were different due to the lower frequency seismic energy source.

2.1.2 Data Processing

The refraction data processing was performed by Advanced Geoscience to prepare seismic velocity profiles along Lines 6, 7, and 8. The field records from selected shot points were input into the RAYFRACT refraction tomography software developed by Intelligent Resources, Inc. (Vancouver, Canada). RAYFRACT was used to generate seismic compressional-wave velocity profiles of the upper 200 feet along each survey line. This refraction tomography modeling procedure is generally more capable of accurately imaging sharper lateral velocity variations due to faulting than other refraction tomography methods and conventional two to five-layer refraction interpretation methods such as the Generalized Reciprocal Method (Sheehan, et al, 2005).

The field records selected from shot points showing more clearly defined first arrival times (“first breaks”) were used to perform RAYFRACT refraction tomography modeling. For Line 6, a total of 31 field records were used with shot points spaced 20 to 90 feet apart. For Line 7, 41 records were used with shot points spaced 30 to 110 feet apart. For Line 8, 65 records were used with shot points spaced 20 to 110 feet apart.

The field records were input into the RAYFRACT program to graphically pick first breaks for refracted waves traveling through the surface layer and into deeper higher-velocity layers. These time-distance data were used together with geophone station coordinates and elevations to conduct refraction tomography imaging of the shallow seismic velocity layering. RAYFRACT was used to first generate an initial velocity-depth model for each line using the Delta TV method. This initial model was then refined to produce a closer fit to the arrival time data using the Wavepath Eikonal Traveltime (WET) inversion method with 60 iterations with a maximum velocity 3,000 m/sec. The best-fit velocity-depth models were then gridded and color contoured with SURFER (written by Golden Software, Inc.) to show estimated vertical and lateral velocity variations. The resulting seismic compressional-wave velocity profiles for Lines 6, 7, and 8 are shown Figures 7, 8, and 9.

The specialized seismic reflection data processing was performed by Advanced Geoscience with considerations given to known structural and stratigraphic geologic conditions. The VISTA 2D seismic reflection data processing software (developed by Gedco in Calgary, Alberta) was used to prepare seismic reflection profiles for Lines 6, 7, and 8. The entire volume of field records for each survey line were input into this computer program together with the measured geophone coordinates and elevations to perform sequences of data editing, digital filtering, trace sorting, velocity corrections, and trace summation to prepare migrated, CMP-stacked, reflection time profiles. Several iterations of this data processing were performed on each survey line and evaluated and modified until a set of processing parameters was arrived at that provided the clearest images of geologic structure and stratigraphy. The resulting migrated reflection time profiles for Lines 6, 7 and 8 are shown in Figures 7, 8 and 9. A more detailed discussion and summary of the procedures used for these profiles is provided in Appendix A.

The significant variations in ground surface elevation along Lines 6, 7 and 8 were also accounted for in the reflection data processing. A refined datum elevation correction procedure was used that first calculated surface-consistent, CMP-referenced, floating datum elevation static (time) shifts which were applied the field record traces (Frei, 1995). The data processing was then carried out through CMP stacking and migration, and after migration the CMP traces were shifted to final horizontal datum elevations. The final time shifts introduced by this step effectively reduced the reference time ($t=0$) on the reflection profiles to horizontal datum planes located above the highest ground surface elevations on the east end of the lines. The datum plane elevations and replacement velocities used for these calculations were as follows:

Line 6 Datum=3,880 feet	$V_{\text{Replacement}}=1,700$ ft/sec
Line 7 Datum=3,880 feet	$V_{\text{Replacement}}=1,700$ ft/sec
Line 8 Datum=3,830 feet	$V_{\text{Replacement}}=1,700$ ft/sec

Figures 7, 8 and 9 show the reflection and refraction profiles along Lines 6, 7 and 8 with the same horizontal scale (1 inch= 200 feet) with the same positioning relative to one another. The vertical scale for the refraction profiles shows subsurface velocity layering at 2:1 vertical exaggeration (1 inch= 100 feet). Note that these

horizontal and vertical scales are different than the scales used for the Phase 1 and 2 profiles. The profiles for Lines 3, 4 and 5 are displayed with horizontal scale of 1 inch= 100 feet, with the vertical scale for the refraction profiles also 1 inch= 100 feet. The longer reflection profiles for Lines 1 and 2 are shown at horizontal scales of 1 inch= 300 feet. The vertical scale for all of the reflection time profiles was adjusted to roughly convey geologic structure at 1:1 vertical to horizontal aspect ratio.

2.2 PHASE 4- SEISMIC REFLECTION AND REFRACTION PROFILING ON LINES 9, 10, AND 11

Advanced Geoscience conducted additional seismic surveys along Lines 9, 10 and 11 from June 7 through 18, 2012. Line 9 was positioned along the axis of the proposed replacement dam and extended to the east to provide subsurface coverage across the right abutment of the dam and the elevated terrace area. Line 10 was positioned along a northwest-to-southeast orientation to better correlate reflection patterns and faulting across Lines 1, 6, 9, and 8. Line 11 was positioned in the canyon area north of Line 5 on the east side of the reservoir to provide a better mapping of the A1-A4 fault planes between Lines 5 and 6 and the connection of this faulting to Fault A.

A higher-output seismic energy source was used for the longer Lines 9 and 10 to overcome background noise from stronger wind conditions which occurred periodically. Line 11 was recorded using the previously-used shotgun shell energy source. This line was positioned in a canyon area where stronger winds were not anticipated to cause a significant noise problem.

2.2.1 Data Collection

Advanced Geoscience first setup stakes at 100-foot intervals along each survey line to establish geophone stationing. These control points mostly followed the traverses setup earlier by LADWP with some slight deviations to position the lines away from areas later identified by the biologist and archeologist field monitors. LADWP land surveyors also later measured the coordinates and elevations of these control points and provided this data to us in a computer spreadsheet file.

The data recording procedures used for Lines 9 and 10 were similar to the procedures used for Lines 6, 7, and 8. However, Line 11 was setup for better near-surface resolution using procedures similar to those used for Line 5 in Phase 2.

The data recording was also conducted using the same Seistronix EX-6 data recording system used in Phases 1 through 3. The EX-6 system was connected to geophone receiver spreads setup along each survey line. Lines 9 and 10 consisted of multiple, overlapping geophone spreads with 126 40-Hertz geophones spaced 10-feet apart. Line 11 consisted of a fixed geophone spread with 120 40-Hertz geophones spaced 8-feet apart. The following lists the total length of geophone coverage setup along each survey line:

Line 9 3,050 feet Line 10 3,050 feet Line 11 952 feet

Lines 9 and 10 were recorded first using a “downhole percussion”, seismic energy source. At each shot point six-inch diameter holes were pre-drilled by a power auger and hand dug to stay open. The holes were dug 2.5 to 3 feet deep. A licensed blaster from Alpha Explosives (in Mojave, California) placed single 200 or 350 gram cast boosters in each hole with seismic fuse wires. The blaster worked together with our survey crew to load and trigger this energy source as the seismic data were recorded along the length of each survey line.

The seismic data were recorded in a west-to-east movement on Lines 9 and 10. A 4WD Polaris Ranger was used to move the drilling equipment, seismic cable, geophones, and recording electronics along the survey lines. The central recording computer was setup inside a 4WD passenger vehicle which was also moved along the survey lines.

Lines 9 and 10 were recorded mostly with shot points positioned at 10-foot intervals. Some shot point locations were skipped, resulting in 20-foot intervals, to avoid environmentally sensitive areas and speed up data production to stay on schedule. Generally, the first shot points started 5-feet west of the first geophone position and continued along the line between each geophone position. Line 10 was recorded first followed by the recording of Line 9.

As the shot points moved to the east, the 126-channel geophone spreads were also shifted to the east in increments of 600-feet. This shift in geophone spread positioning was generally made after the shot points moved 300-feet past the centerline of each geophone spread. This walk through 126-channel geophone recording configuration generated reflection datasets along Lines 9 and 10 with maximum 50 to 80-fold subsurface coverage with 5-foot CMP reflection spacing.

The resulting surveys recorded a total of 279 field records for Line 9 and 272 field records for Line 10. Each 126-channel field record was recorded with an 800 millisecond record length and 0.25 millisecond sampling rate with 24 bit analog-to-digital resolution.

Line 11 was setup last at the end of the field program and recorded with the shotgun shell seismic energy source. The seismic waves were generated using a Betsy Seisgun to fire single 400-grain shotgun shell blanks beneath the ground in shallow auger borings 2 to 3 feet deep. At each shot point location two shotgun shell blanks were separately fired and the recordings from each firing were summed together to increase the amplitude of reflections and cancel out random background noise from stronger wind gusts.

The data was recorded with shot points positioned along the line at 8-foot intervals. The seismic vibrations from each shot point were recorded into the fixed 120-channel geophone spread with geophones spaced 8-feet apart. The first shot points started 4-feet west of the first geophone position and continued along the line between each geophone position. The last shot point was positioned at station 860 feet. Due to stronger wind gusts, we did not continue recording data to the end of this 952-foot long survey line. This decision was made to avoid processing poorer quality data from the

east end of the line with higher quality data recorded over most of the line.

The fixed, 120-channel geophone recording configuration used on Line 11 generated a reflection dataset with maximum 95-fold subsurface coverage near the center of the spread with 4-foot CMP reflection spacing for higher resolution.

The survey along Line 11 recorded a total of 101 field records. Each 120-channel field record was recorded with an 800 millisecond record length and 0.25 millisecond sampling rate with 24 bit analog-to-digital resolution.

The data recording for Lines 9 and 10 provided mostly higher quality field records. The recording along Line 11 also provided higher quality field records over most of the length of the line. However, as noted above, poorer quality records were recorded on the last 160 feet of the line where we experienced noise from stronger wind vibrations occurring later in the day.

2.2.2 Data Processing

The field records from several shot points were input into RAYFRACT to generate seismic compressional-wave velocity profiles along Lines 9, 10, and 11. Records were selected from shot points showing more clearly defined first breaks to perform this refraction tomography modeling. For Line 9, a total of 42 field records were used with shot points spaced 50 to 90 feet apart. For Line 10, 44 records were used with shot points 40 to 80 feet apart. For Line 11, 19 records were used with shot points 16 to 56 feet apart.

Using the same procedures in Phase 3, the field records were input into RAYFRACT to graphically pick first breaks. These time-distance data were used together with geophone station coordinates and elevations to first generate an initial velocity-depth model for each line using the Delta TV method. This initial model was then refined to produce a closer fit to the arrival time data using the Wavepath Eikonal Traveltime (WET) inversion method with 60 iterations with a maximum velocity 3,000 m/sec. The best-fit velocity-depth models were then gridded and color contoured with SURFER to show estimated vertical and lateral velocity variations. The resulting seismic compressional-wave velocity profiles for Lines 9, 10, and 11 are shown Figures 10, 11, and 12.

The VISTA 2D seismic reflection processing software was also used to prepare seismic reflection profiles for Lines 9, 10, and 11. The volume of field records for each survey line were input into this computer program with measured geophone coordinates and elevations to perform data processing steps similar to those used in Phase 3 to prepare migrated, CMP-stacked, reflection time profiles. Several iterations of this data processing were performed on each survey line to generate the clearest reflection images of geologic structure and stratigraphy. (Appendix A includes a more detailed discussion and summary of these processing procedures.)

The significant variations in ground surface elevation along Lines 9, 10 and 11

were also accounted for using the same procedures used in Phase 3. Final static time shifts were introduced that effectively reduced the reference time ($t=0$) on the reflection profiles to horizontal datum planes located above the highest ground surface elevations on the east end of the lines. The datum plane elevations and replacement velocities used for these calculations were as follows:

Line 9 Datum=3,880 feet	$V_{\text{Replacement}}=1,700$ ft/sec
Line 10 Datum=3,880 feet	$V_{\text{Replacement}}=1,700$ ft/sec
Line 11 Datum=3,930 feet	$V_{\text{Replacement}}=2,000$ ft/sec

The datum elevation and $V_{\text{Replacement}}$ for Lines 9 and 10 were kept the same as those used in the processing for Lines 6 and 7 in Phase 3. This provided more accurate ties of the reflection horizons and fault plane interpretations at points where these lines intersected Line 10.

The reflection data from Line 9 was processed first as soon as the survey coordinates and elevations were provided to us by LADWP. A preliminary CMP-stacked reflection time profile was prepared to provide an initial interpretation of the possible faulting beneath Line 9 along the axis of the proposed dam. This preliminary interpretation was provided to URS in July, 2012 to help select locations for sonic boreholes to be drilled on the axis of the dam.

The reflection data for Line 9 was later reprocessed together with the processing for Lines 10 and 11 to prepare the final migrated reflection time profiles shown in Figures 10, 11, and 12. Additional reprocessing was also conducted of the Phase 3 data for Lines 6, 7, and 8 to see if these reflection profiles could be enhanced for better imaging of fault planes. Figure 7 shows the enhanced reflection time profile generated for Line 6.

The reflection and refraction profiles for Lines 9 through 11 are shown in Figures 10 through 11 with the same horizontal scale and positioning relative to one another. These profiles are displayed with a horizontal scale of 1 inch= 200 feet, with the vertical scale for the refraction profiles showing subsurface velocity layering at a 2:1 vertical exaggeration (1 inch= 100 feet). The vertical scale for the reflection time profiles was also adjusted to roughly convey geologic structure at 1:1 vertical to horizontal aspect ratio.

3.0 DISCUSSION OF RESULTS

3.1 GEOLOGIC INTERPRETATION OF SEISMIC PROFILES AND EVALUATION OF SUBSURFACE FAULTING

3.1.1 Phases 1 and 2

The seismic reflection profiles for Lines 1 and 2 provided the first images of deeper basin structure and faulting beneath the area. The interpretation of these profiles

in Figures 2 and 3 revealed a thin layer of alluvium overlying sequences of Tertiary-age layering extending to depths of 4,000 to 5,000 feet. Both profiles showed deeper, west-sloping reflections interpreted as the possible metamorphic or granitic basement. Above these basement reflections were reflection patterns indicating Tertiary sedimentary layering and possible volcanic sequences. This layering appeared to dip mostly to the west toward a lower elevation point in the basin graben west of the survey area.

The higher-resolution, shallower-imaging seismic reflection profiles for Lines 3 and 4 in Figures 4 and 5 also revealed similar reflection patterns from west-dipping Tertiary layering.

Several reflection patterns showing similar amplitude, phase, and time-depth structure were first interpreted across Lines 1 through 4. These reflections appeared to be from similar-age geologic horizons and were used as marker horizons for the evaluation of faulting. These reflection patterns were labeled as R1 through R4 on the profiles. Our current interpretation of these reflection patterns is summarized below.

- The R1 reflection pattern is interpreted to be the upper surface of the Pliocene Coso Formation (Tc) bedrock. This reflection pattern is identified in several areas by truncated reflections above and below this horizon which appear to mark the alluvium-Coso Formation bedrock unconformity. In some areas this unconformity surface is not a well resolved reflection horizon due to the weaker seismic impedance contrast between the alluvium and weathered bedrock surface and interference caused by the water table reflection and refraction patterns. However, the positioning of this R1 reflection horizon on Lines 1 and 3 is consistent with the bedrock profile interpreted from lithologic logs from boreholes drilled near the dam by LADWP (2007). (Figures 2 and 4 show the alluvium-Coso Formation contact from these boreholes approximately projected into the seismic profiles based on an approximate depth-to-travel time conversion.)
- The R2 reflection identifies a stronger-amplitude, continuous reflection pattern from a harder bedding surface within the upper part of the Coso Formation.
- The R3 reflections appear to be from deeper conformable bedding surfaces in the Coso Formation.
- The deeper R4 reflections could be associated with the top and bottom surfaces of a volcanic layer near the bottom of the basin that eventually thins out to the west.

The first clear evidence of subsurface faulting was detected on Line 1. Fault planes projecting upward towards the surface were obvious on Line 1 between CMPs 120 and 200 in Figure 2. These fault planes were interpreted based on similar patterns of vertical offset observed on the R2 through R4 reflections.

After the Phase 2 surveys were completed a more detailed interpretation of faulting on Lines 1 through 4 revealed two consistent patterns of faulting. The near-surface projections of these fault traces were initially labeled A1 through A3 and C1 through C3 on Lines 1 through 4. Each of these fault planes was interpreted based on their alignment along multiple vertical offsets or sharp changes in dip on the R1-R4 reflection horizons.

The current interpretation of subsurface layering and faulting on the reflection time profiles for Lines 1 through 4 is shown in Figures 2 through 5. This interpretation was revised to be consistent with the interpretation shown on the Phase 3 and 4 profiles (discussed below). The clear patterns of fault plane deformation on these profiles are shown by the solid black lines. Less certain patterns are shown by dashed black lines. Older (deeper) fault planes within the Tertiary section are shown by dashed blue lines.

As discussed in our earlier report, the fault planes interpreted on Lines 1 and 3 show the primary justification for separating the “A faults” from the “C faults”. These two fault patterns appear to extend downward to the basement along two separate vertical paths. In addition, the A1 and A2 faults are characterized by east-dipping fault planes with mostly down-to-the-east separation and sharp changes in dip on the R1 through R4 reflection horizons. The C1 and C2 faults are characterized by more vertical fault planes near the surface with older deformation that does not appear to extend much above the upper surface of the R2 green reflection horizon. The C1 and C2 faults also show a deeper pattern of vertical offset and change in dip on the R2, R3, and R4 reflections. The previously identified faults labeled A3 and C3 are now omitted from our current interpretation of faulting and no longer considered to be separate fault planes. Our revised interpretation of the Line 4 reflection profile (Figure 5) shows the C3 fault omitted and C2 fault below the R2 reflection horizon.

The reflection and refraction profiles for Line 3 (Figure 4) show better near-surface resolution of this faulting. The A1, C1, and C2 faults all create sharp changes in dip along the R2 and R3 reflection horizons. These changes in dip occur along east-dipping fault planes. Previously, the C1 fault on Line 3 was interpreted to extend above the R2 reflection horizon to the bedrock surface. This interpretation was based on the sharp bedrock high point shown by the R1 reflection pattern and the juxtaposition of the 6,500 ft/sec velocity layering near the middle of Line 3, which indicated a possible fault-emplaced bedrock high. This bedrock high point is now interpreted to be caused by the bedrock ridge line extending into the subsurface which is shown on the site map in Figure 1 north of LADWP Borehole PH 86-2. Faults C1 and C2 on Line 3 now appear to show older deformation in the Coso Formation that does not extend much above the upper surface of the R2 green reflection horizon.

The positioning of Line 5 to the south adjacent to Fault A (where it was discovered by trenching) helped characterize the seismic expression of Fault A. The reflection and refraction profiles for Line 5 (Figure 6) show Fault A to be associated with

an east-dipping fault plane which is now believed to connect with the A2 fault pattern. The A2 fault on Line 5 shows down-to-the-east separation on the R1 bedrock reflection and the 5,500 to 6,500 ft/sec velocity layering on the refraction profile, which is interpreted as the bedrock surface. The A2 fault plane also shows this down-to-the-east separation on the deeper R2 reflection as well as a sharp change in the direction of dip on the R3 reflection. Note that the A2 and A4 faults on Line 5 show more obvious vertical offset near the surface. At greater depths these fault planes show less obvious vertical offset and are revealed more by sharp changes in the direction of reflector dip, similar to the A1, C1, and C2 faults on Line 3. This apparent decreased vertical offset with depth could be due partly to the time scale's vertical representation of these profiles, which near the surface results in an increased vertical depth scale due to the lower seismic velocities.

It is noted that the current trenching completed by URS in 2012 revealed a similar pattern of vertical separation for the faulting associated with Fault A. Their observations reported primarily down-to-the-east separations and that Fault A is mostly an east-dipping fault plane similar to A2 fault.

The Phase 1 and 2 profiles also revealed no evidence of near-surface faulting outside of the bounds of the A1-A4 faults and C1-C2 faults. The seismic reflection profiles along Lines 1 and 2 showed no patterns of faulting projecting upward toward the surface on the west side of the valley north of the dam. In addition, no evidence of subsurface faulting was detected on the east end of the profiles which could create the prominent north-south topographic escarpment referred to as the "Miscellaneous East Fault" (Figure 1).

3.1.2 Phase 3 and 4

The seismic reflection profiles from the Phase 3 and 4 surveys show R1 through R3 reflection patterns which are similar in amplitude and time-depth structure to those first identified on Lines 1 through 4 from the Phase 1 and 2 surveys. In addition, other reflection patterns are also identified such as the water table reflection in the valley alluvium and an older alluvial surface beneath the elevated terrace area to the east. These reflection patterns are identified on the profiles for Lines 6 through 11 (in Figures 7 through 12). Our interpretation of these reflection horizons on the seismic profiles is also tied at the points where Line 10 intersects Lines 1, 7, 8, and 9.

The down hole percussion energy source used for the Phase 4 surveys produced the clearest reflection images on the profiles for Lines 9 and 10. These enhanced reflection images were helpful in re-interpreting the reflection patterns interpreted on Lines 6, 7, and 8 from the Phase 3 surveys. As previously reported, the energy source used for the Phase 3 surveys caused the frequency and phase characteristics of these reflection patterns to be different. The overall coherency of these reflection patterns was also degraded by noise interference from the strong winds experienced during the Phase 3 surveys. To help improve reflection coherency a second migration procedure was performed in the final data processing for Lines 7 and 8. This migration procedure

did improve the overall reflection coherency, but it also degraded higher-frequencies and caused some upward sweeping patterns on the edges of the reflection profiles.

The reflection profiles for Lines 9 and 10 provided the best evidence of the A faults and C faults previously interpreted. The fault planes interpreted on these profiles were similar to the patterns first interpreted on reflection profiles for Lines 1 and 2 in Phase 1. These reflection profiles showed similar east-dipping A1, A2, and C1 fault planes that were extended to the reflection profiles for Lines 6, 7, and 8.

The A1 and A2 faults on these profiles are now interpreted to define an east-tilted fault block which extends from Line 6 to the north across Line 2. These A1-A2 faults also appear to show deformation which is younger than the C1-C2 faults. The A1 fault plane extends above the R2 reflection horizon to the R1 bedrock interface reflection. The A2 fault plane extends above the R1 reflection pattern into the older alluvium. Evidence of this alluvial deformation is also shown on the refraction profiles for Lines 6, 7, and 8 by abrupt changes in the 3,000 to 5,000 ft/sec velocity layering which indicates deformation above the bedrock alluvium interface.

The A4 and A5 fault planes interpreted to the east on Lines 5, 6, and 11 also show deformation above the R1 bedrock reflection with abrupt changes in velocity on the refraction profiles, which could suggest younger faulting to the east.

The C1 and C2 fault planes which were first interpreted on the reflection profiles for Lines 1 and 3 appear to be older patterns of deformation within the Coso Formation that terminate to the north. The reflection profile for Line 9 shows that the C1 fault does not extend above the R2 reflection horizon. To the north of Line 9 this fault plane also appears to merge with the A1 fault. The vertical separation of the C2 fault is close to our limit of detection on the reflection profiles for Lines 4 and 9. However, there is evidence of a consistent pattern of deformation that indicates this fault plane extends from Lines 1 and 3 to the northwest across the reflection profiles for Lines 4, 7, 8 and 9. The deformation associated with this C2 fault plane also does not appear to extend above the R2 reflection horizon.

The recent sonic boreholes drilled on Line 9 along the axis of the proposed replacement dam and its east abutment support our interpretation that the C1 and C2 faults are older fault planes within the Coso Formation. These borings were drilled into the upper part of the Coso Formation bedrock and used to develop a geologic cross section of two identifiable marker beds, designated as the upper and lower marker beds. The locations of these boreholes are shown on Figure 13 which shows an enlarged (1 inch= 100 feet) scale view of the Line 9 reflection profile across the east abutment area. To show the positioning of the bedrock-alluvium contact and the two marker beds the measured depths of these interfaces were converted to the seismic travel time shown on the vertical axis of this profile using velocities from the refraction tomography profile. Figure 13 shows the estimated travel time positioning of these marker beds on Line 9. Note that the uppermost reaches of the C1 and C2 fault planes are stratigraphically below these two west-dipping marker beds and within an older part of the Coso Formation.

Fault A discovered in the trenches along the eastern shoreline of the reservoir is now interpreted to extend to the north as the A2 fault plane from Line 5 to Line 2. The recent trenching north of Line 5 indicates that Fault A trends to the north. This alignment is consistent with a similar alignment of the A2 and A4 faults which can be extended to the south from Lines 6 and 11 to Line 5. The profiles for Lines 6 and 11 show A2 and A4 fault planes that reveal a localized down-dropped, pull-apart, fault block similar to the one first interpreted on Line 5.

The profiles for Lines 4, 7, 8, and 9 also show reflection patterns and seismic velocity variations near the surface which indicate ancient river channeling beneath the east side of the valley. This channeling appears to have cut into the upper part of the Coso Formation.

3.2 MAPPING OF TREND OF SUBSURFACE FAULTING

The site map in Figure 1 shows the positioning of the A1-A5 faults and C1-C2 faults on Lines 1 through 11 and our current interpretation of the trend of the upper trace of these fault planes across the area.

The mapping in Figure 1 indicates the A1-A5 faults are the more dominant fault patterns that continue to the north and south beneath the area. The A2 fault is located east of the existing dam and the proposed replacement dam and appears to connect to Fault A discovered in the trenches immediately north of Line 5. This connection is based on the recent trenching observations and the pattern of A2-A4 faulting interpreted on Lines 5, 6, and 11.

The mapping also shows the revised trend of the older C1 and C2 faults. The C1 fault is located east of the abutment of the proposed replacement dam and is shown to merge to the north with the A1 fault. The C2 fault trends to the northwest beneath the valley and crosses the alignment of the proposed replacement dam. The deformation associated with the C2 fault does not appear to extend above the R2 reflection horizon which is below the elevation of the marker beds identified in the recent sonic boreholes.

3.3 EVALUATION OF FAULT PLANE DETECTION LIMIT

The reflection profile from Line 9 on the axis of the dam was used to evaluate a detection limit for vertical separation caused by a fault plane. The weaker pattern of deformation shown by the C2 fault on Line 9 appears to be close to this detection limit. In our interim reporting it was first reported that the C2 fault was not detected on Line 9; however, after a closer evaluation it appears there exists a slight vertical offset and change in dip in multiple reflection patterns along a vertical fault plane consistent with the trend of the C2 fault (Figure 13). In addition, weaker-amplitude, steeply-dipping events indicating diffracted waves are visible along this fault plane. The VISTA 2D processing software was used to create an enlarged window of this area on the Line 9

reflection profile. Using the average travel time offset of 2.5 milliseconds across the C2 fault plane immediately below the R2 reflection horizon and an estimated “interval velocity” of 6,000 ft/sec, an estimate was made of the vertical separation associated with this faulting. This evaluation indicated a vertical separation of 7.5 feet at the depth of the R2 reflection. If this same amount of travel time offset were extended to the R1 bedrock-alluvium reflection the interval velocity of 5,000 ft/sec in this area would indicate a vertical offset of about 6 feet at this depth. This evaluation suggests that a vertical separation due to faulting of 5 feet or less may not be detectable in the bedding planes near the bedrock alluvium contact.

The primary features used in the detection of fault planes on seismic reflection profiles are the alignment of travel time offsets and changes in dip along near-vertical or inclined pathways through multiple reflection patterns. Patterns of diffracted waves, decreased reflection amplitudes beneath the fault plane (fault shadow), and fault plane reflections (which are rarely observed) are also good secondary features for the detection of fault planes (Liner, 1999). The interpretation of subsurface faulting shown in this report is based mostly on the alignment of travel time offsets, changes in dip, and diffraction patterns, and the similar occurrence of these fault plane features on multiple, paralleling seismic reflection profiles.

4.0 REFERENCES

Bradford, et al., 2006, Imaging complex structure in shallow seismic-reflection data using prestack depth migration, *Geophysics*, volume 71, no. 6, Society of Exploration Geophysicists, November-December 2006.

Frei, 1995, Refined field static corrections in near-surface reflection profiling across rugged terrain, *The Leading Edge*, Society of Exploration Geophysicists, April, 1995.

LADWP, 2007, North Haiwee Reservoir Geologic Investigation, City of Los Angeles Department of Water and Power, April, 2007.

Liner, 1999, *Elements of 3D Seismology*, PennWell Publishing, 1999.

Sheehan et al., 2005, An evaluation of methods and available software for seismic refraction tomography, *Journal of Environmental and Engineering Geophysics*, volume 10, Environmental and Engineering Geophysical Society, March 2005.

URS Corporation, 2007, Preliminary Local Fault Investigations for Proposed North Haiwee Dam Number 2 (Draft Report), December, 20, 2007.

Yilmaz, 2001, *Seismic Data Analysis, Processing, Inversion, and Interpretation of Seismic Data, Volume 1*, Society of Exploration Geophysicists, 2001.

APPENDIX A

SEISMIC REFLECTION DATA PROCESSING PROCEDURES

This appendix describes the processing procedures used by Advanced Geoscience to generate the final migrated seismic reflection time sections for Lines 6 through 11. These procedures were implemented using the VISTA 2D seismic reflection processing software (developed by Gedco in Calgary, Alberta). More information on these standard processing procedures can be found in geophysical exploration references on seismic data processing such as that by Yilmaz (2001).

The processing procedures described below were implemented and graphically displayed in VISTA to evaluate their influence in improving the resolution of reflections. Where necessary, these parameters were changed and the processing steps were repeated to improve this resolution.

In addition to the elevation static time shifts described in the main part of this report, “residual static” time shifts were also applied. This “stack power” analysis procedure was used to statistically calculate small static shifts which were applied to the normal moveout (NMO) velocity-corrected common midpoint (CMP) traces to improve the coherency of the stacked section. These corrections helped remove some of the time shifts caused by smaller-scale, near-surface velocity variations.

Multiple steps of velocity analysis between dip moveout (DMO) corrections, residual static corrections, and pre-stack time migration (PSTM) processing were applied based on the procedures recommended by Yilmaz (2001). These steps helped incrementally improve the coherency of reflection patterns. The PSTM processing also helped reposition dipping reflections up dip to their more correct CMP location. Our experience and the experience of others (Bradford, et al., 2006) indicates that pre-stack migration on common-offset panels is a better migration procedure for near-surface seismic reflection data versus conventional post-stack time migration.

The following lists the general sequences of processing procedures used on the reflection data sets recorded in the Phase 3 and 4 surveys.

Lines 7 and 8

1. Field record editing to remove bad records
2. Geometry definition
3. 2D crooked line common-midpoint (CMP) binning
4. Re-sampling from 0.25 ms to 0.5 msec sample rate
5. Traced editing
6. Triggering static corrections to remove bulk delays
7. Exponential amplitude enhancement for spherical divergence correction
8. Time variant scaling for trace amplitude recovery

9. FK filtering to attenuate steeply dipping noise
10. Band pass filtering
11. Automatic gain control (AGC) using 150 ms windows to restore trace amplitude
12. Predictive deconvolution for wavelet compression and multiple attenuation
13. Final trace muting of refraction events
14. CMP elevation static shifts- surface to smoothed floating datum
15. Time variant spectral balancing and RMS scaling
16. Initial velocity analysis using semblance and corrected CMP gathers
17. Normal moveout (NMO) correction using initial velocity functions
18. Initial CMP stacking and reflection profile display
19. CMP elevation static shifts- floating datum to final datum plane
20. Dip move out (DMO) corrections
21. CMP elevation static shifts- final datum plane back to floating datum
22. Inverse NMO correction and second velocity analysis
23. NMO correction using second velocity analysis
24. Residual static corrections using stack power analysis
25. Inverse NMO correction and third velocity analysis
26. NMO correction using third velocity analysis
27. FK Pre-stack time migration (PSTM) on common-offset panels
28. Inverse NMO correction and final velocity analysis
29. NMO correction using final velocity analysis
30. Final CMP stacking
31. Final band pass filtering
32. AGC using 100 msec window
33. FX prediction filtering
34. Post-stack FK migration using smoothed PSTM velocities
35. CMP elevation static shifts- floating datum to final datum plane
36. Bandpass filtering
37. Three trace averaging using 0.5,1,0.5 weighting
38. AGC using 150 ms windows for final display
39. FX prediction filtering for final display

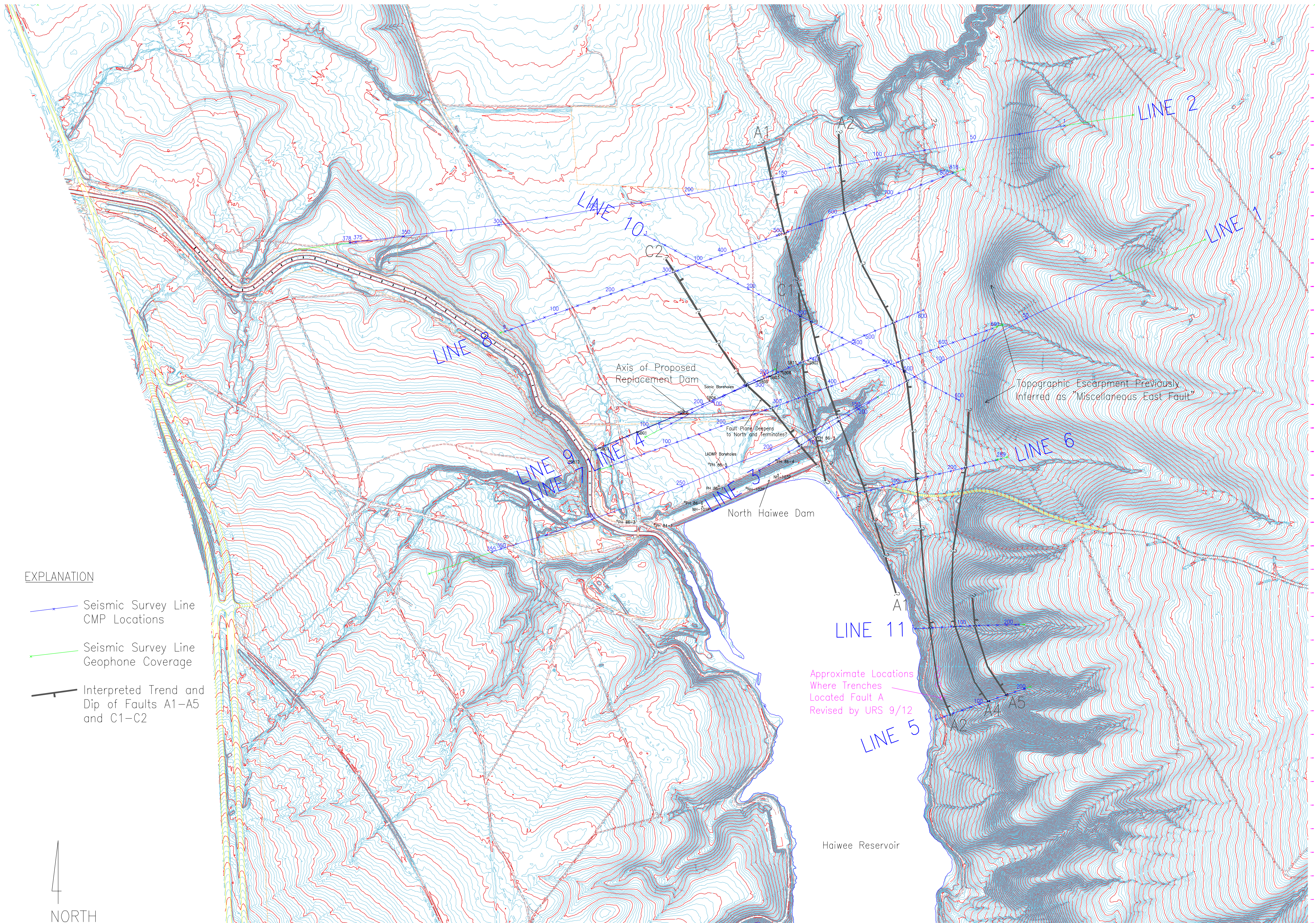
The second post-stack FK migration procedure (in step 34) was performed in the final data processing for Lines 7 and 8 to improve the overall coherency of reflections. This additional processing was needed due to the higher-level of background noise interference from strong wind gusts and the lower-frequency, mixed phase content of the seismic energy source. However, this processing also degraded higher-frequencies and caused some upward sweeping patterns on the edges of the reflection profiles.

Lines 6, 9, 10 and 11

1. Field record editing to remove bad records
2. Geometry definition
3. 2D crooked line common-midpoint (CMP) binning
4. Re-sampling from 0.25 ms to 0.5 msec sample rate
5. Traced editing

6. Triggering static corrections to remove bulk delays (Line 6 only)
7. Exponential amplitude enhancement for spherical divergence correction
8. Time variant scaling for trace amplitude recovery
9. FK filtering to attenuate steeply dipping noise
10. Band pass filtering
11. Automatic gain control (AGC) using 150 ms windows to restore trace amplitude
12. Predictive deconvolution for wavelet compression and multiple attenuation
13. CMP elevation static shifts- surface to smoothed floating datum
14. Final trace muting of refraction events
15. Time variant spectral balancing and RMS scaling
16. Initial velocity analysis using semblance and corrected CMP gathers
17. Normal moveout (NMO) correction using initial velocity functions
18. Initial CMP stacking and reflection profile display
19. CMP elevation static shifts- floating datum to final datum plane
20. Dip move out (DMO) corrections
21. CMP elevation static shift- final datum plane back to floating datum
22. Inverse NMO correction and second velocity analysis
23. NMO correction using second velocity analysis
24. Residual static corrections using stack power analysis
25. Inverse NMO correction and third velocity analysis
26. NMO correction using third velocity analysis
27. FK Pre-stack time migration (PSTM) on common-offset panels
28. Inverse NMO correction and final velocity analysis
29. NMO correction using final velocity analysis
30. Final CMP stacking
31. Final band pass filtering
32. Three trace averaging using 0.5,1,0.5 weighting
33. AGC using 100 ms windows for final display
34. CMP elevation static shift- floating datum to final datum plane
35. FX prediction filtering for final display (Lines 6 and 11 only)

The final FX prediction filtering was not used for Lines 9 and 10 due to the higher quality of this data. However, this processing was used for Lines 6 and 11 to improve reflection coherency due the higher-levels of background noise interference from stronger wind gusts.



EXPLANATION

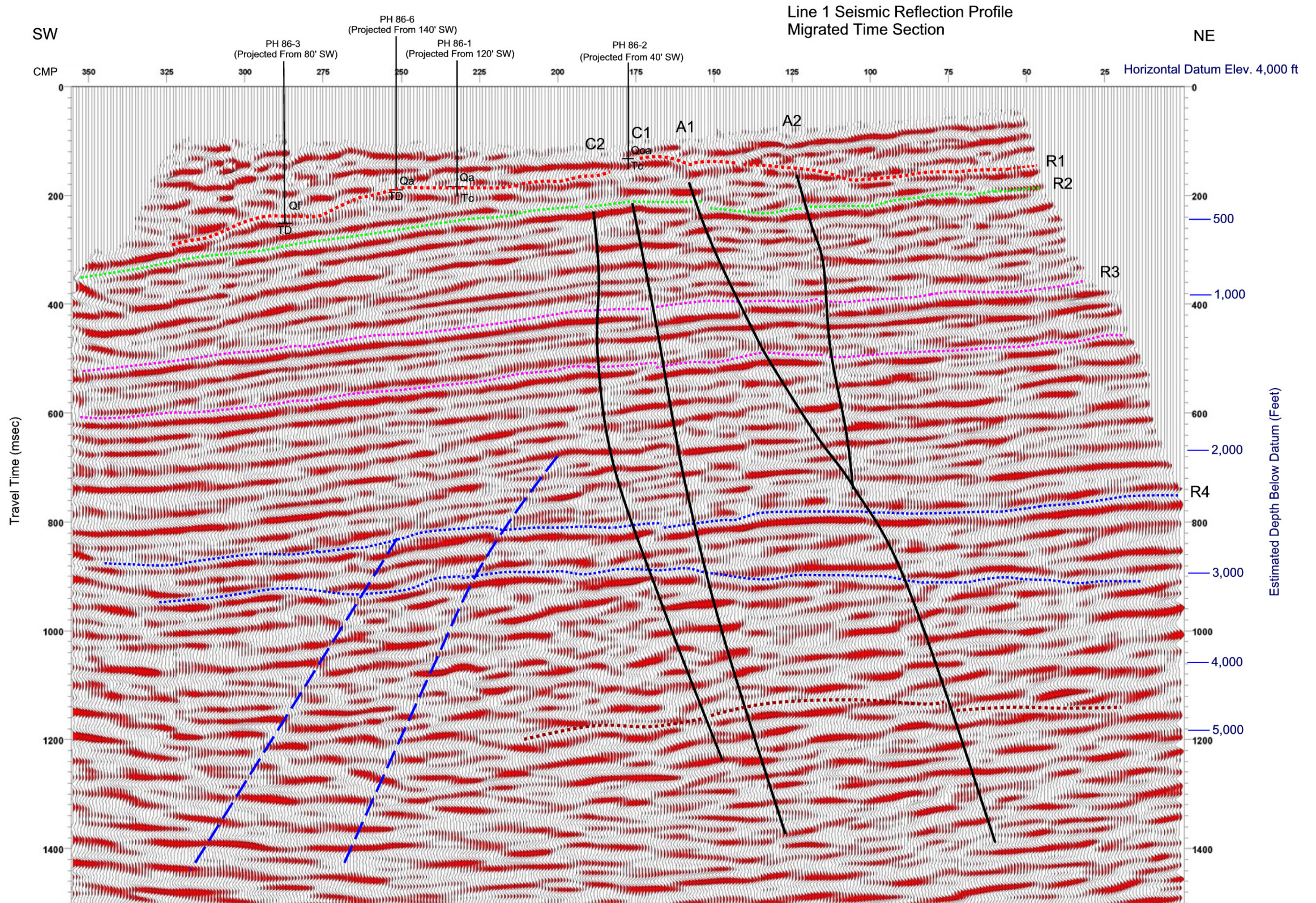
-  Seismic Survey Line
CMP Locations
-  Seismic Survey Line
Geophone Coverage
-  Interpreted Trend and
Dip of Faults A1-A5
and C1-C2



Scale 1 inch= 400 Ft
Base Topographic Site Map Provided by LADWP

PHASE 1-4 SEISMIC SURVEY LINE LOCATIONS AND INTERPRETATION OF SUBSURFACE FAULTING
North Haiwee Dam, Inyo County, California

Figure 1
Advanced Geoscience, Inc.
October, 2012 Revision 8



Horizontal Scale 1 inch= 300 ft

Lithologic Information from Selected LADWP Boreholes
Projected into Profile to Aid Interpretation of Bedrock Surface Reflection.
Positioning of Lithologic Contacts Estimated Based on
Approximate Travel Time-to-Depth Conversion.

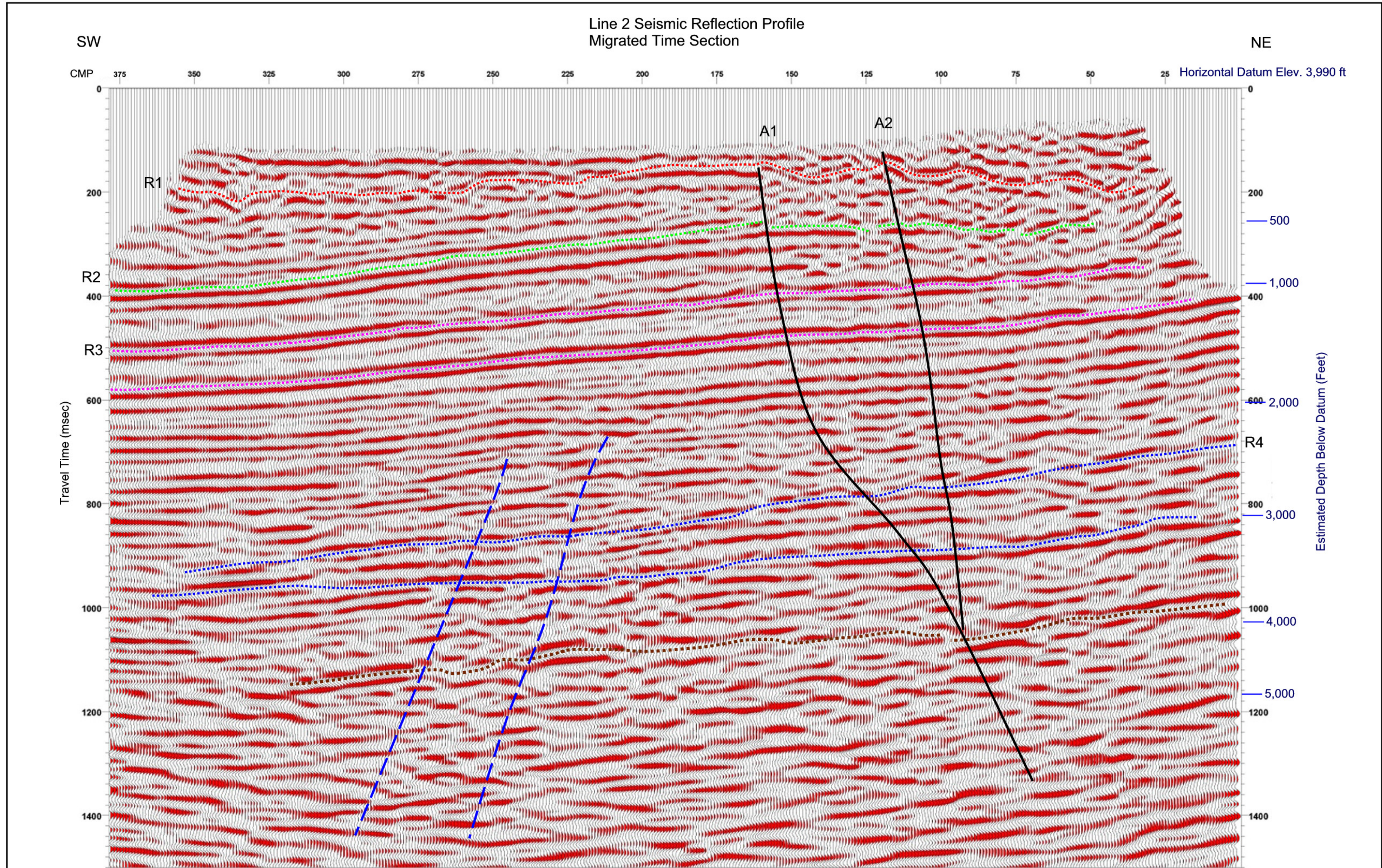
Revised Interpretation 9/12

Interpretation of Seismic Reflection Patterns:

- Pliocene Coso Formation (Tc) Bedrock Surface (R1)
- Coso Formation Bedding (R2)
- Deeper, Conformable Tertiary Bedding (R3)
- Possible Volcanic Layer Thinning to the West (R4)
- Basement Surface

Line 1 Seismic Reflection Profile
Showing Interpretation of Subsurface Layering and Faulting
LADWP North Haiwee Dam
Inyo County, California

Figure 2
Advanced Geoscience, Inc.



Horizontal Scale 1 inch= 300 ft

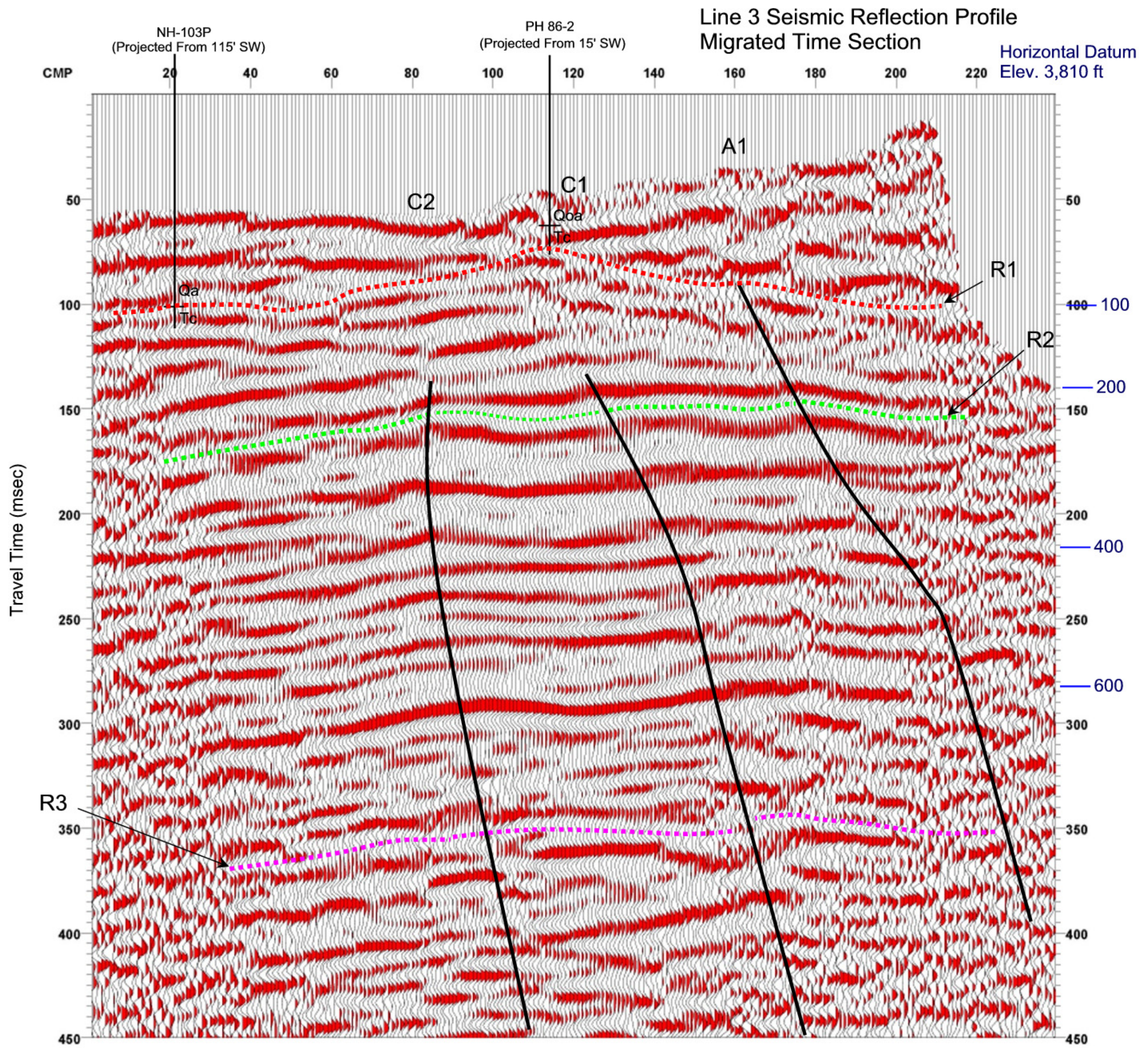
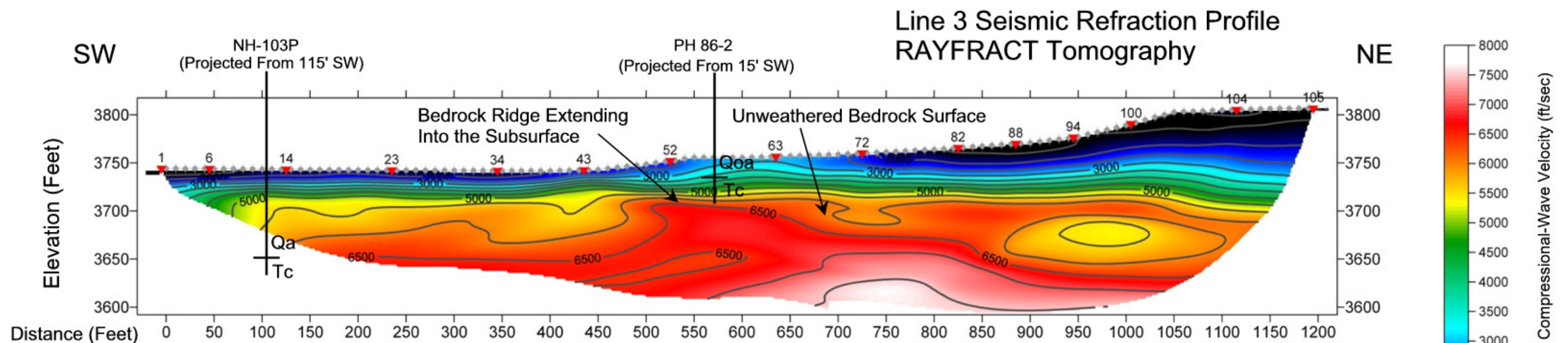
Revised Interpretation 10/12

Interpretation of Seismic Reflection Patterns:

- Coso Formation (Tc) Bedrock Surface (R1)
- Coso Formation Bedding (R2)
- Deeper, Conformable Tertiary Bedding (R3)
- Possible Volcanic Layer Thinning to the West (R4)
- Basement Surface

Line 2 Seismic Reflection Profile
Showing Interpretation of Subsurface Layering and Faulting
LADWP North Haiwee Dam
Inyo County, California

Figure 3
Advanced Geoscience, Inc.



Profiles Shown at Same Horizontal Positioning
 Horizontal Scale 1 inch= 100 ft
 Vertical Scale Refraction 1 inch= 100 ft

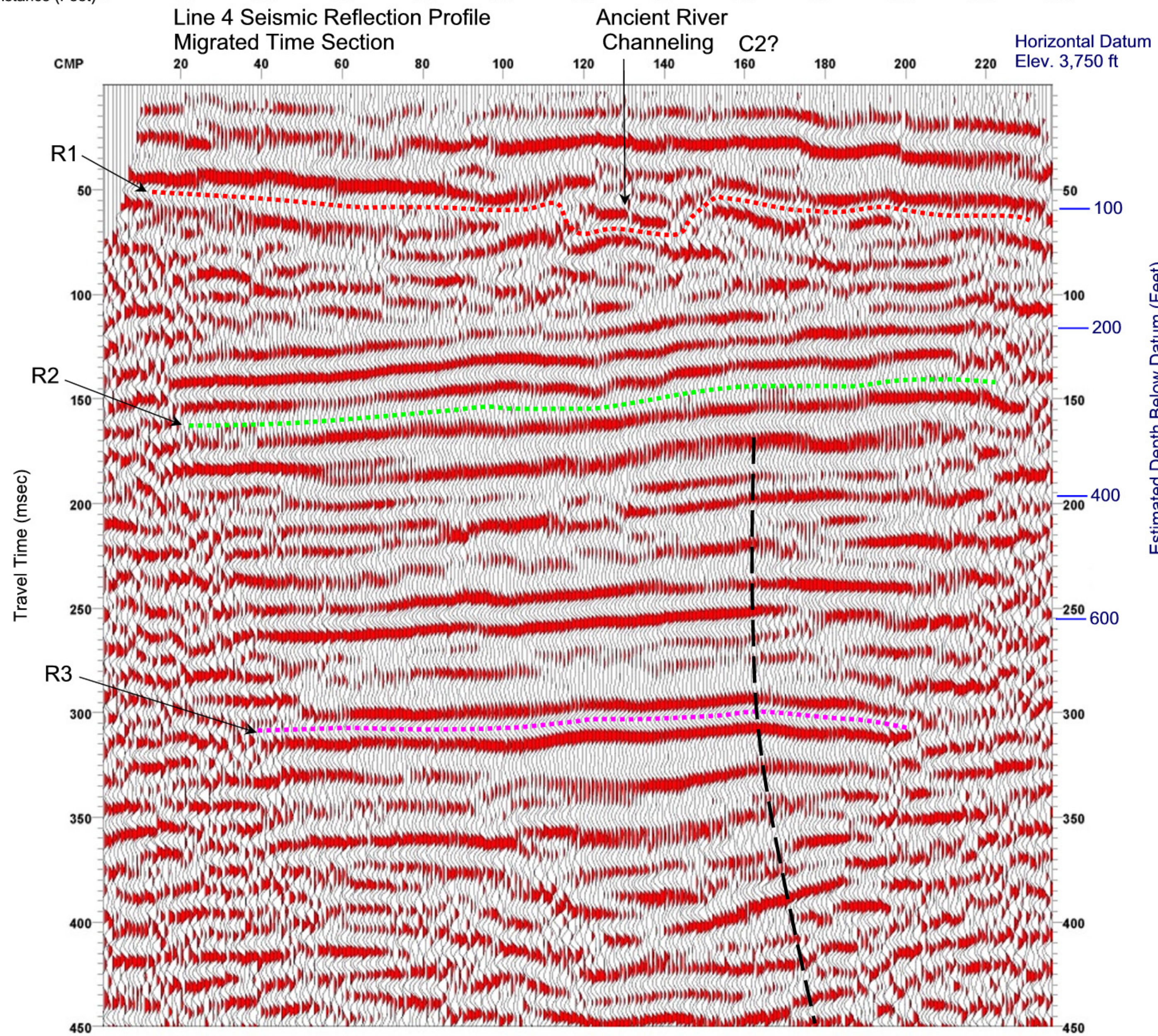
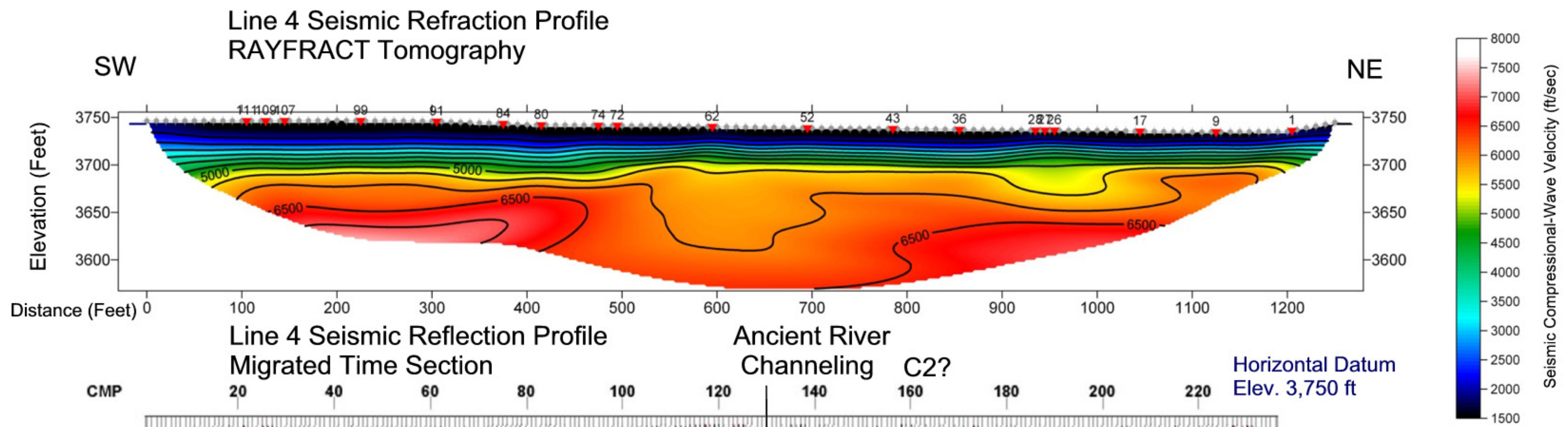
Lithologic Information from Selected LADWP Boreholes
 Projected into Profile to Aid Interpretation of Bedrock Surface Reflection.
 Positioning of Lithologic Contacts Estimated Based on
 Approximate Travel Time-to-Depth Conversion.

- Interpretation of Seismic Reflection Patterns:
- Pliocene Coso Fm. (Tc) Bedrock Surface (R1)
 - Coso Formation Bedding (R2)
 - Deeper, Conformable Tertiary Bedding (R3)

Revised Interpretation 10/12

Line 3 Seismic Reflection and Refraction Profiles
 Showing Interpretation of Subsurface Layering and Faulting
 LADWP North Haiwee Dam
 Inyo County, California

Figure 4
 Advanced Geoscience, Inc.



Profiles Shown at Same Horizontal Positioning
Horizontal Scale 1 inch= 100 ft
Vertical Scale Refraction 1 inch= 100 ft

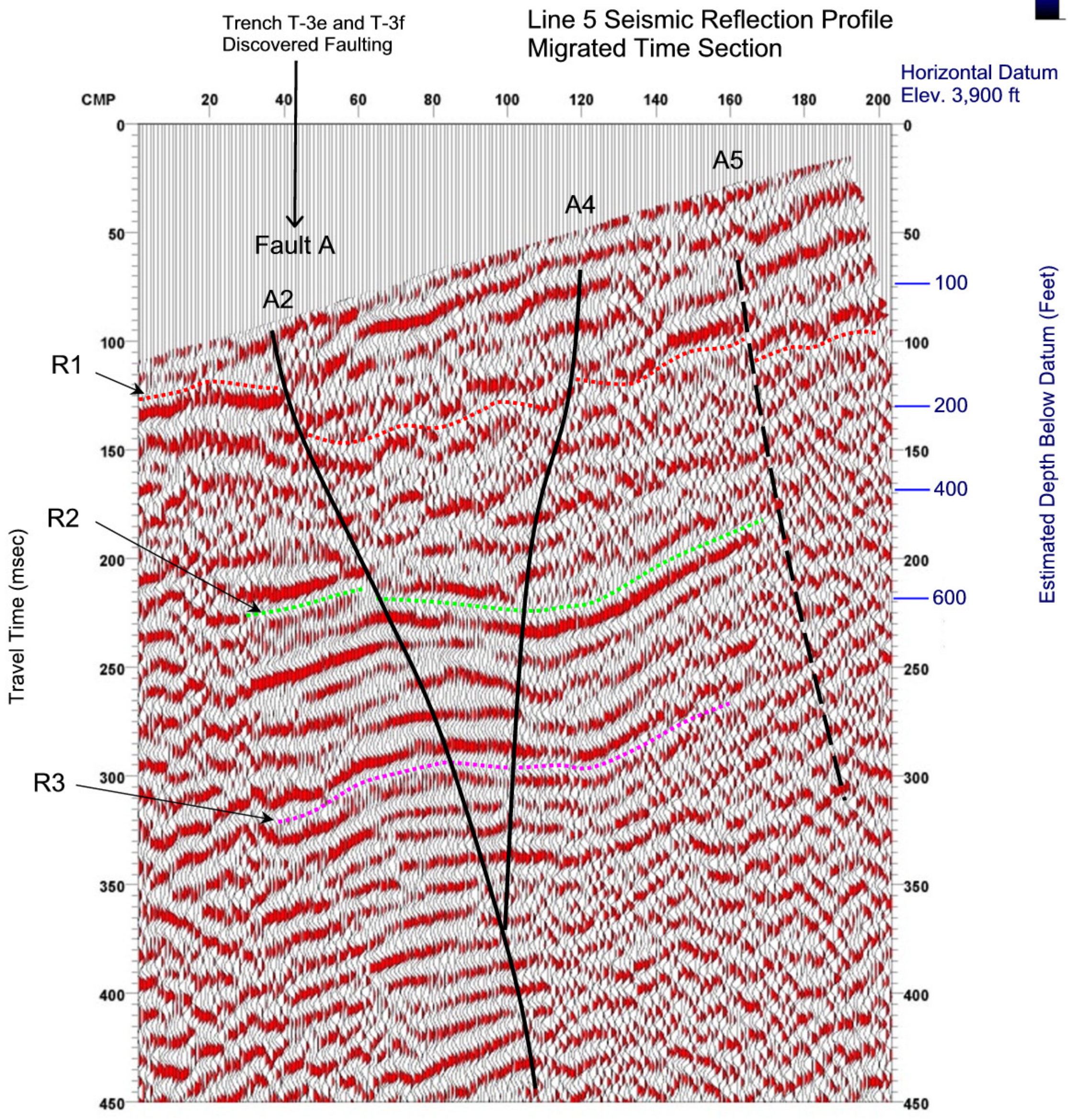
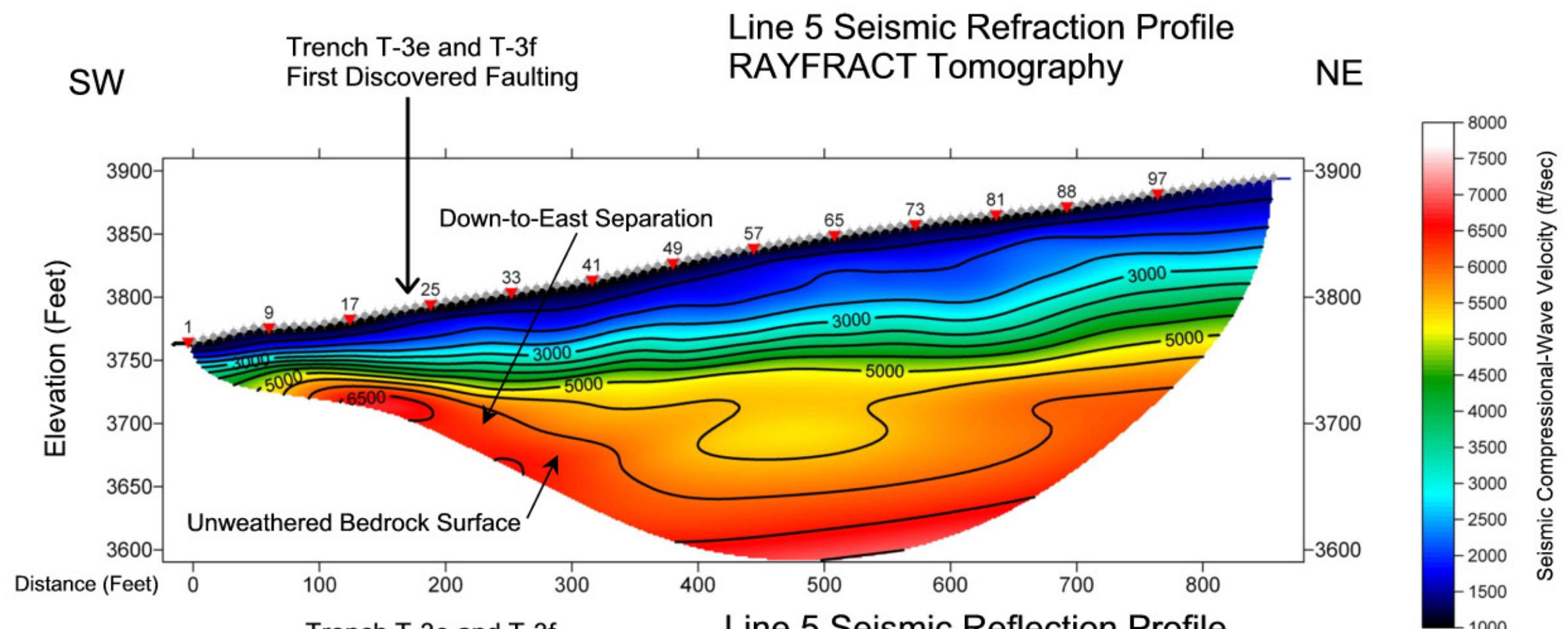
Revised Interpretation 10/12

Interpretation of Seismic Reflection Patterns:

- - - - - Pliocene Coso Formation (Tc) Bedrock Surface (R1)
- - - - - Coso Formation Bedding (R2)
- - - - - Deeper, Conformable Tertiary Bedding (R3)

Line 4 Seismic Reflection and Refraction Profiles
Showing Interpretation of Subsurface Layering and Faulting
LADWP North Haiwee Dam
Inyo County, California

Figure 5
Advanced Geoscience, Inc.

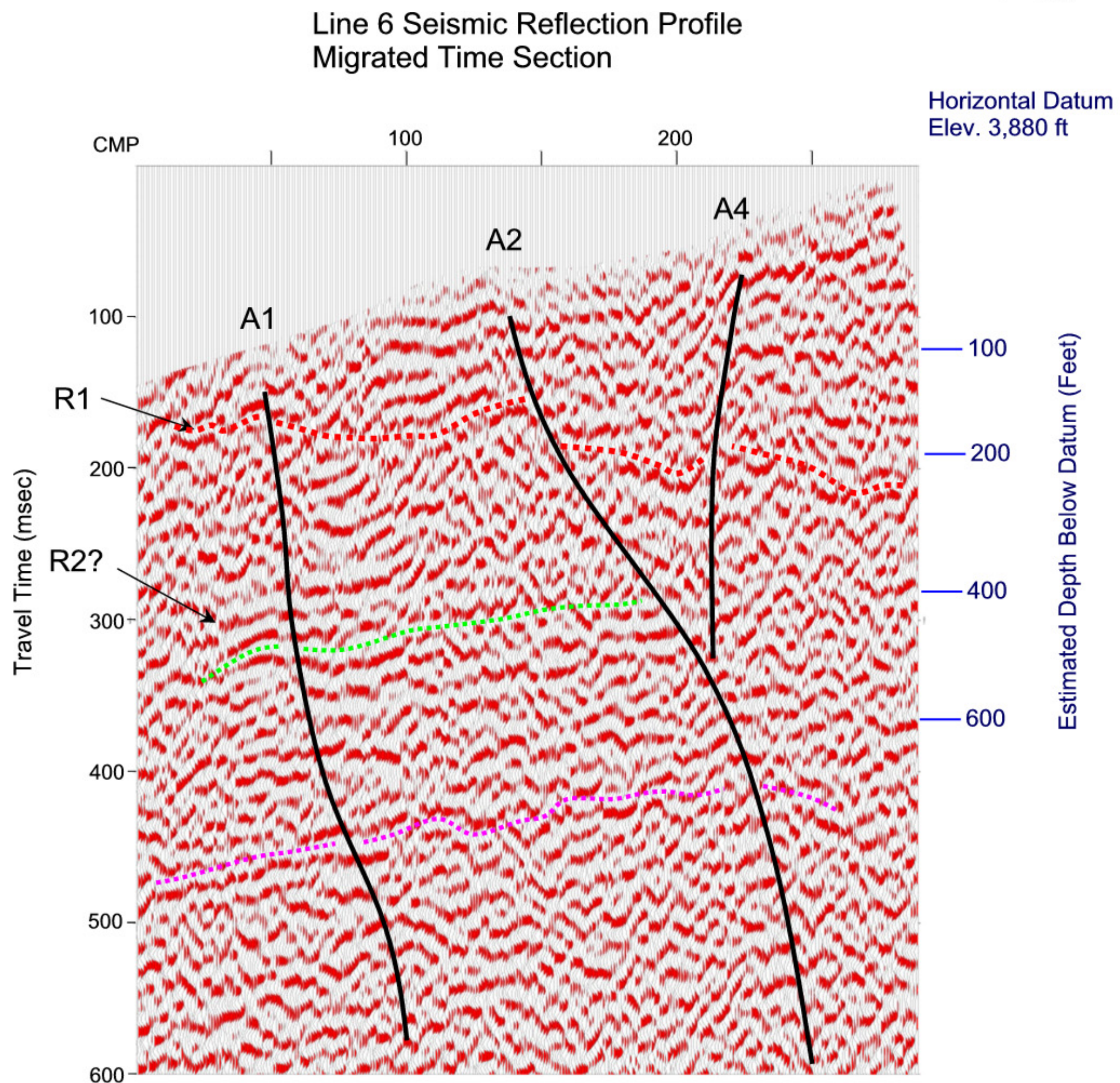
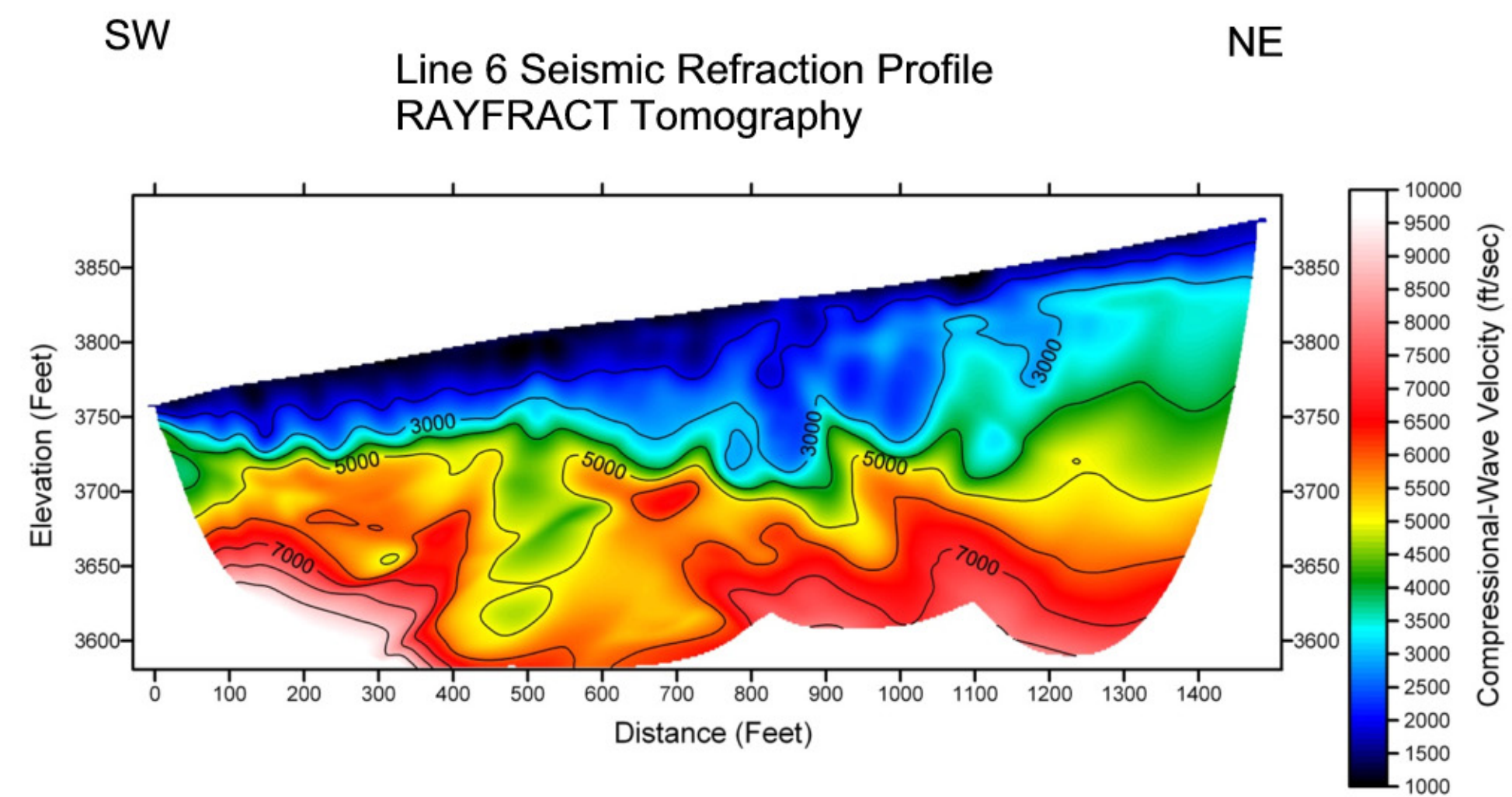


Profiles Shown at Same Horizontal Positioning
 Horizontal Scale 1 inch= 100 ft
 Vertical Scale Refraction 1 inch= 100 ft
 Revised Interpretation 9/12

Interpretation of Seismic Reflection Patterns:
 Pliocene Coso Formation (Tc) Bedrock Surface (R1)
 Coso Formation Bedding (R2)
 Deeper, Conformable Tertiary Bedding (R3)

Line 5 Seismic Reflection and Refraction Profiles
 Showing Interpretation of Subsurface Layering and Faulting
 LADWP North Haiwee Dam
 Inyo County, California

Figure 6
 Advanced Geoscience, Inc.

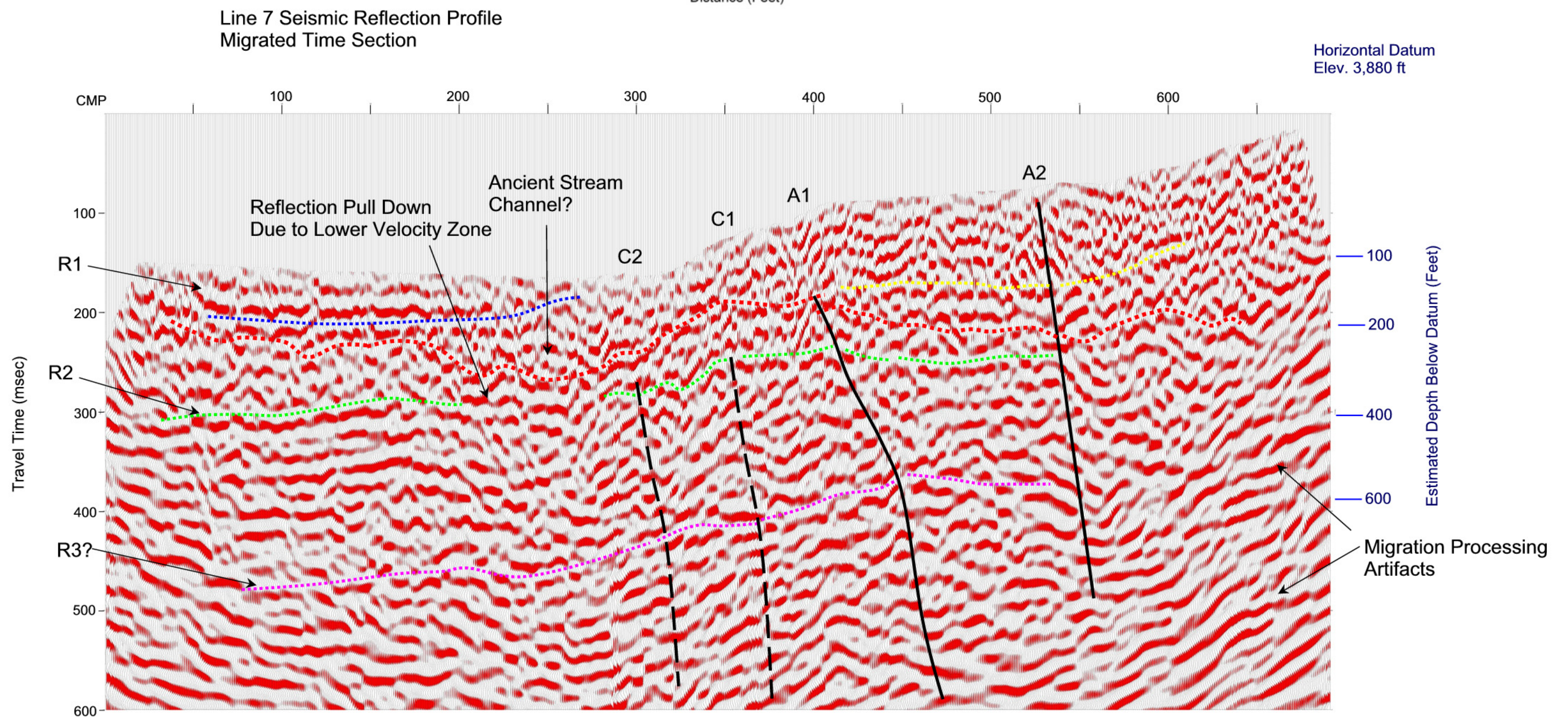
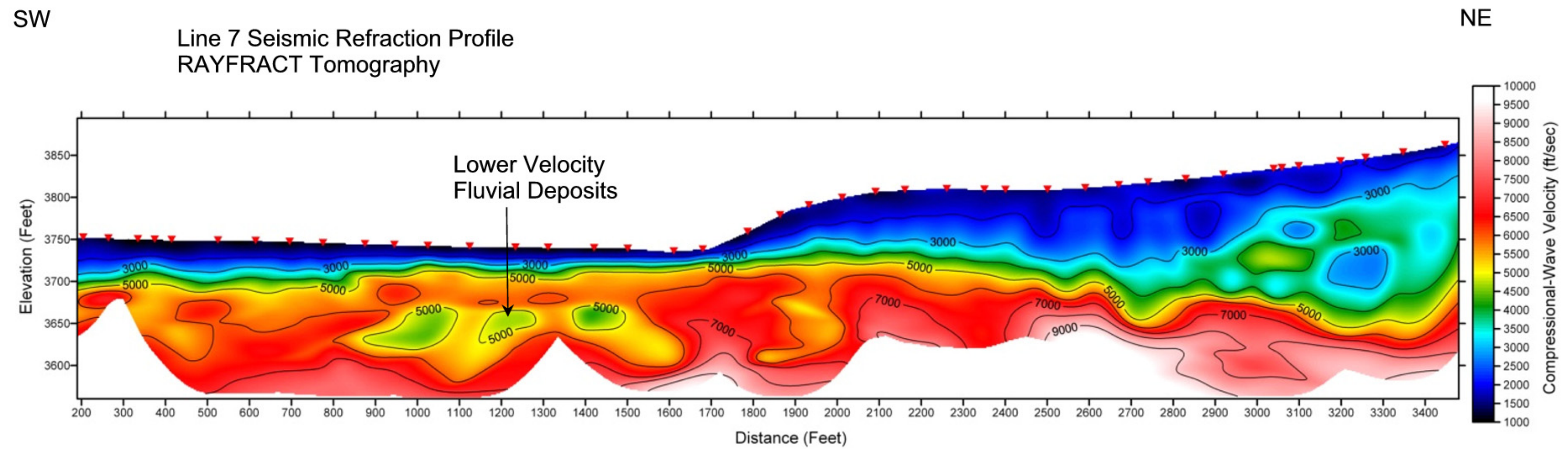


Profiles Shown at Approximate Same Horizontal Positioning
 Horizontal Scale 1 inch= 200 ft
 Vertical Scale Refraction 1 inch= 100 ft (Vertical Exaggeration x 2)

Revised Processing and Interpretation 9/12

- Interpretation of Seismic Reflection Patterns:
- Pliocene Coso Formation (Tc) Bedrock Surface (R1)
 - Coso Formation Bedding (R2)
 - Deeper, Conformable Tertiary Bedding (R3)

Line 6 Seismic Reflection and Refraction Profiles
 Showing Interpretation of Subsurface Layering and Faulting
 LADWP North Haiwee Dam
 Inyo County, California



Interpretation of Seismic Reflection Patterns:

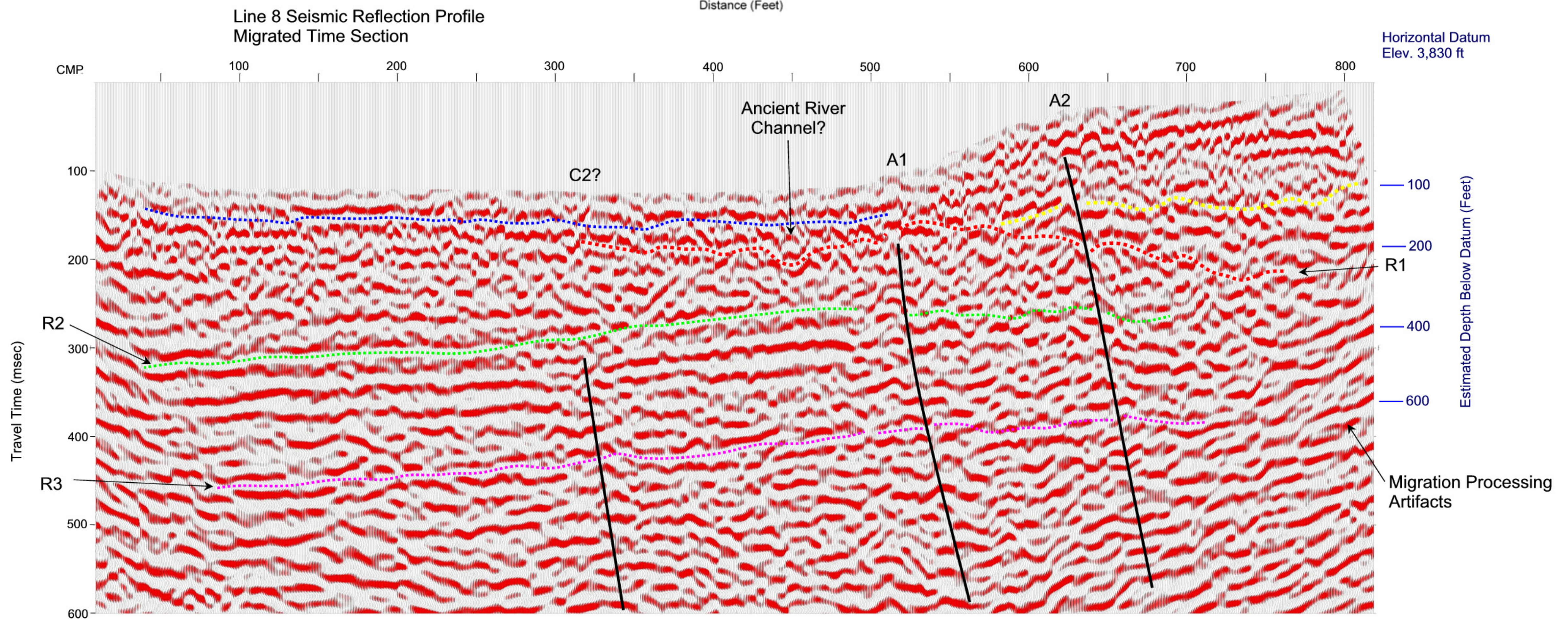
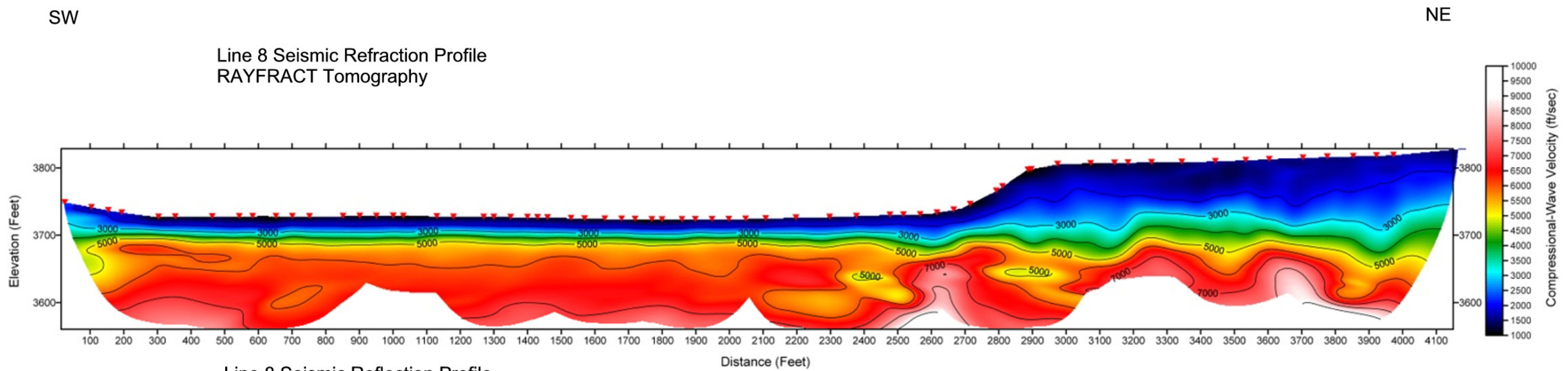
- Valley Alluvium Water Table
- Older Alluvial Surface
- Pliocene Coso Formation (Tc) Bedrock Surface (R1)
- Coso Formation Bedding (R2)
- Deeper, Conformable Tertiary Bedding (R3)

Profiles Shown at Same Approximate Horizontal Positioning
Horizontal Scale 1 inch= 200 ft
Vertical Scale Refraction 1 inch= 100 ft (Vertical Exaggeration x 2)

Line 7 Seismic Reflection and Refraction Profiles
Showing Interpretation of Subsurface Layering and Faulting
LADWP North Haiwee Dam
Inyo County, California

Revised Interpretation 9/12

Figure 8
Advanced Geoscience, Inc.



- Interpretation of Seismic Reflection Patterns:
- Valley Alluvium Water Table
 - Older Alluvial Surface
 - Pliocene Coso Formation (Tc) Bedrock Surface (R1)
 - Coso Formation Bedding (R2)
 - Deeper, Conformable Tertiary Bedding (R3)

Profiles Shown at Same Approximate Horizontal Positioning
 Horizontal Scale 1 inch= 200 ft
 Vertical Scale Refraction 1 inch= 100 ft (Vertical Exaggeration x 2)

Revised Interpretation 10/12

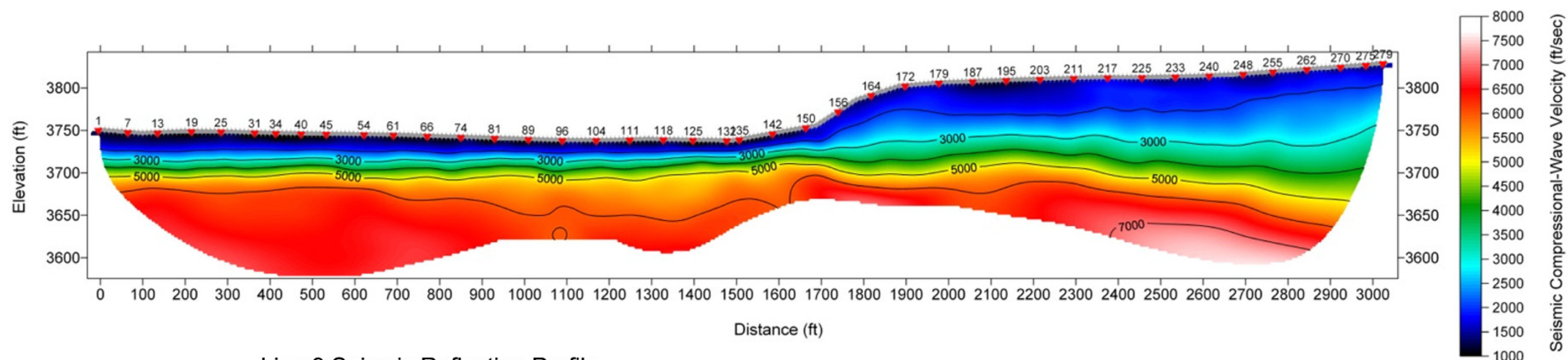
Line 8 Seismic Reflection and Refraction Profiles
 Showing Interpretation of Subsurface Layering and Faulting
 LADWP North Haiwee Dam
 Inyo County, California

Figure 9
 Advanced Geoscience, Inc.

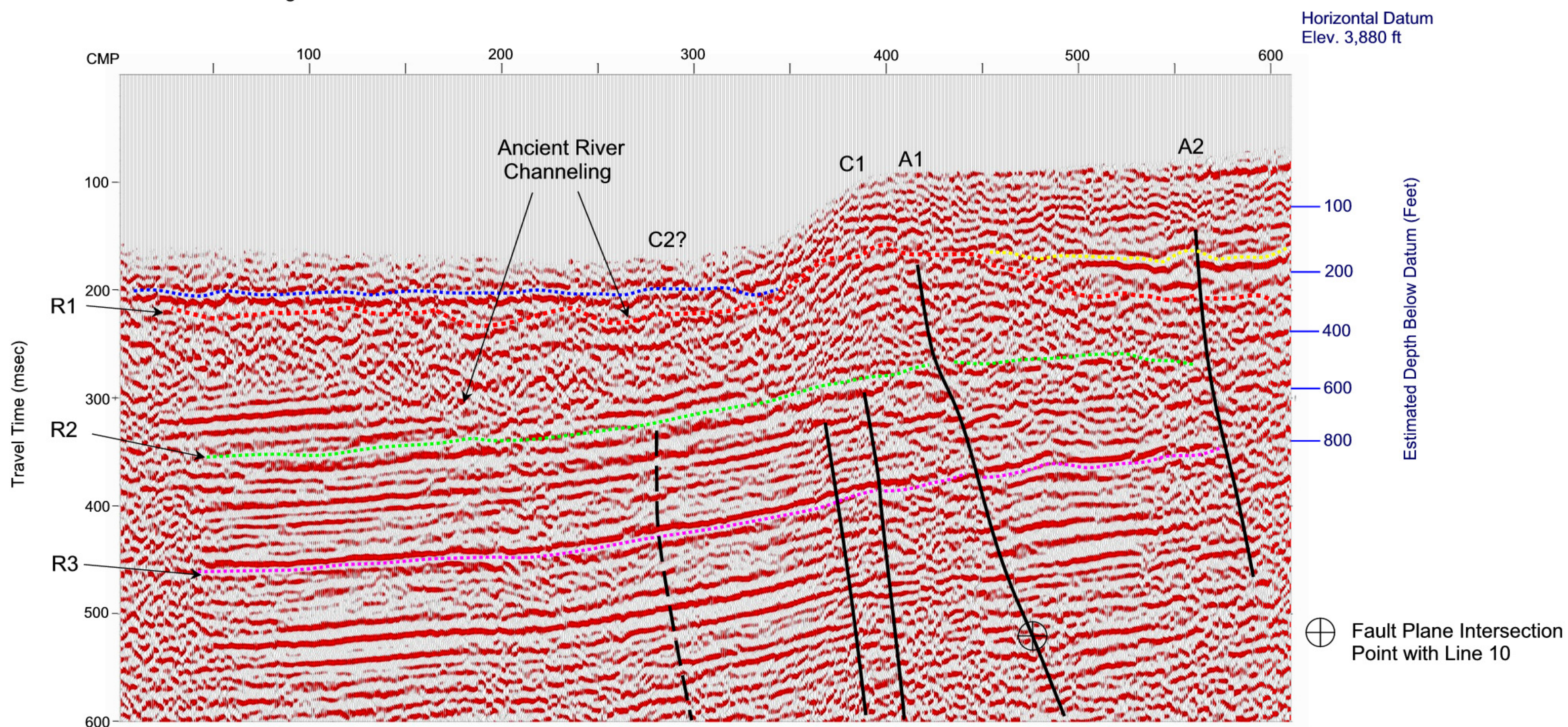
SW

Line 9 Seismic Refraction Profile RAYFRACT Tomography

NE



Line 9 Seismic Reflection Profile Migrated Time Section



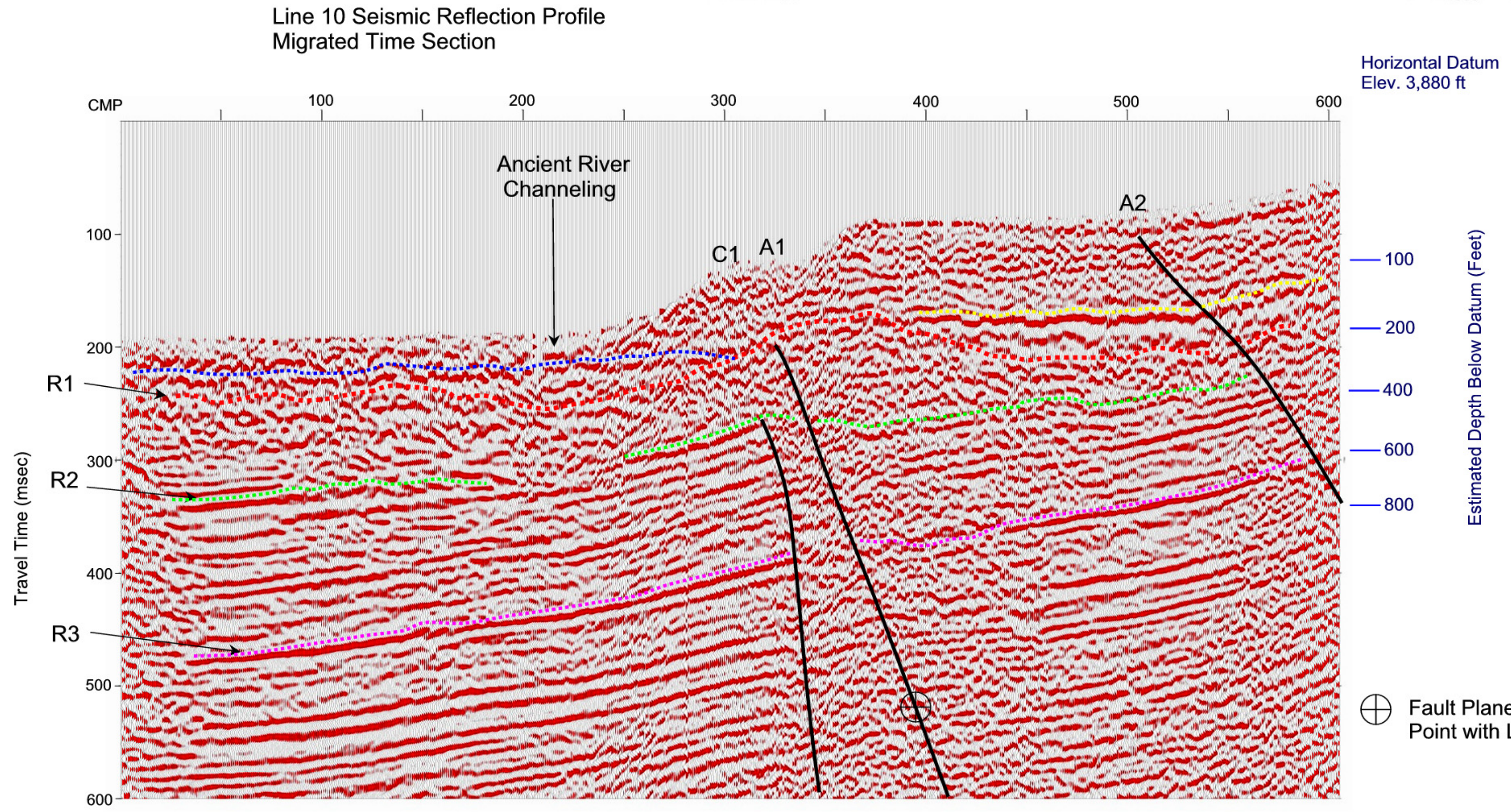
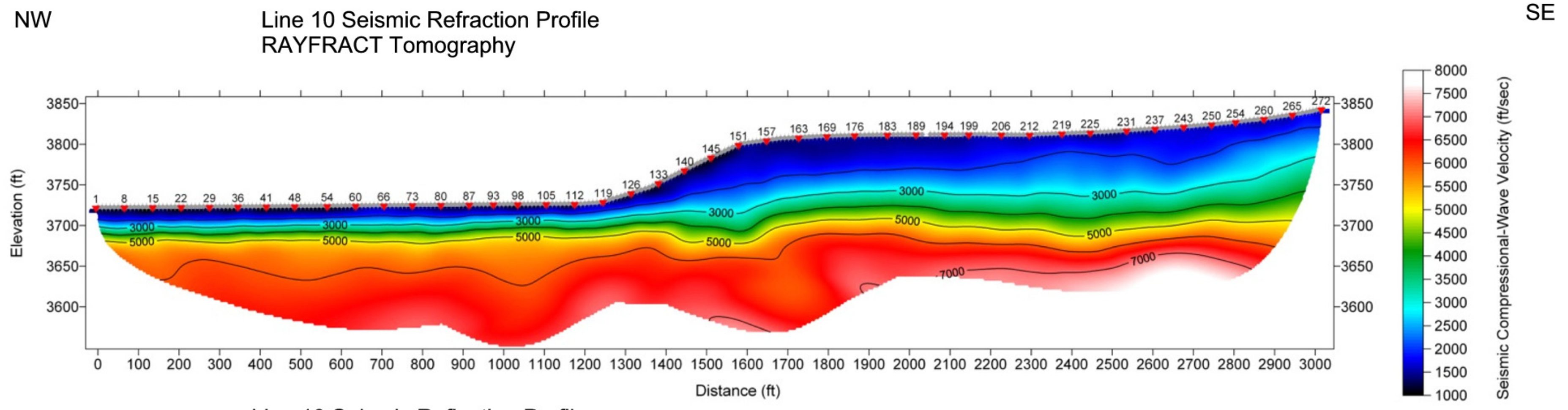
Interpretation of Seismic Reflection Patterns:

- Valley Alluvium Water Table
- Older Alluvial Surface
- Pliocene Coso Formation (Tc) Bedrock Surface (R1)
- Coso Formation Bedding (R2)
- Deeper, Conformable Tertiary Bedding (R3)

Profiles Shown at Same Approximate Horizontal Positioning
 Horizontal Scale 1 inch= 200 ft
 Vertical Scale Refraction 1 inch= 100 ft (Vertical Exaggeration x 2)

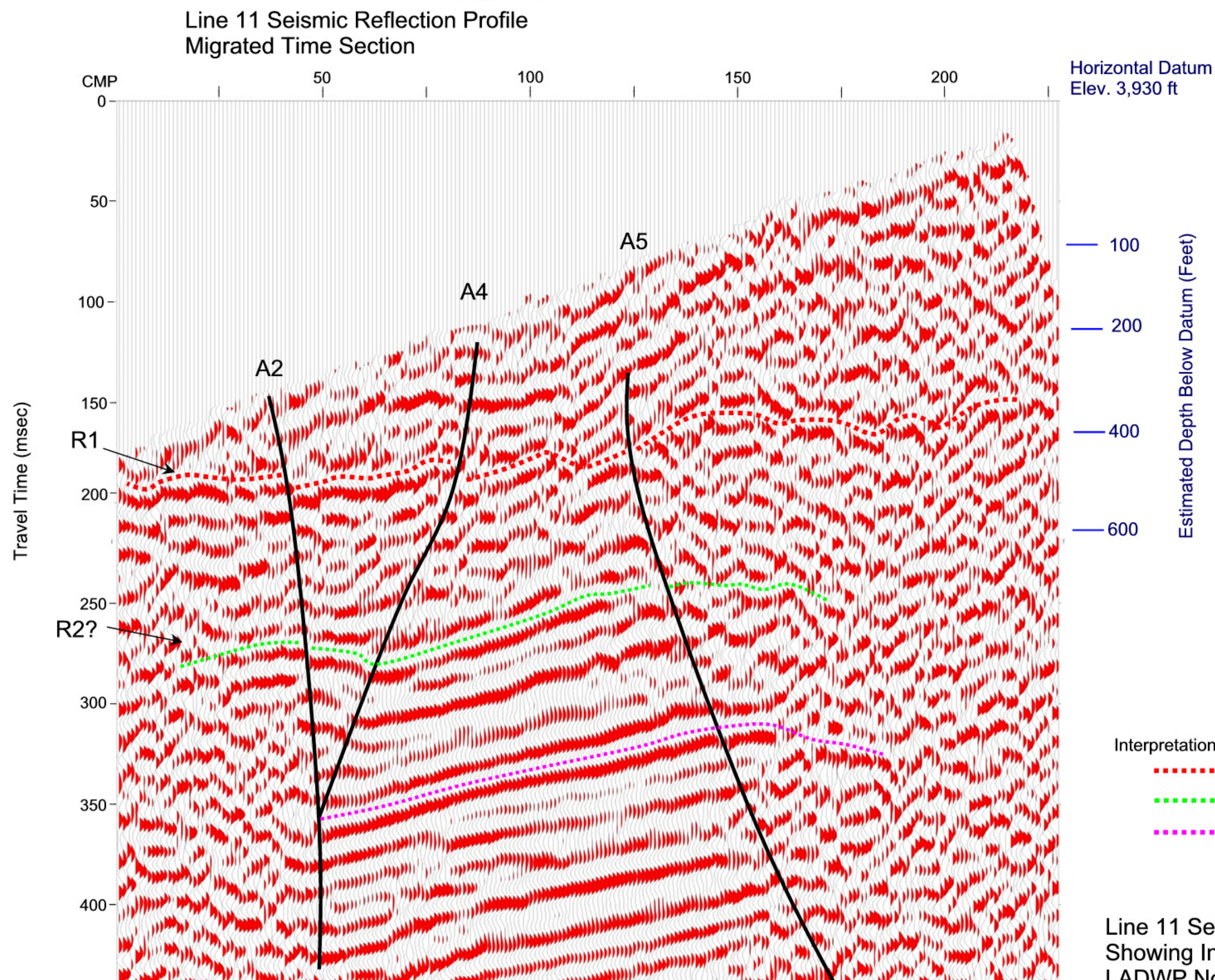
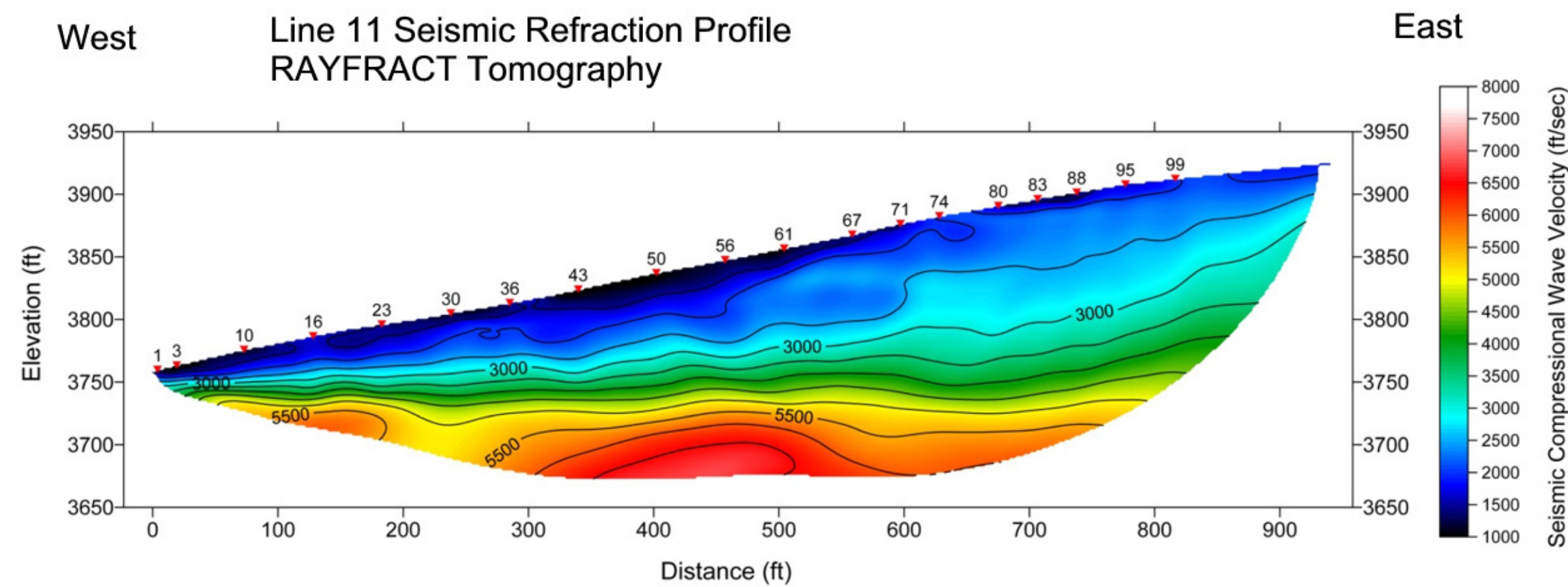
Line 9 Seismic Reflection and Refraction Profiles
 Showing Interpretation of Subsurface Layering and Faulting
 LADWP North Haiwee Dam
 Inyo County, California

Revised Interpretation 10/12



Profiles Shown at Same Approximate Horizontal Positioning
Horizontal Scale 1 inch= 200 ft
Vertical Scale Refraction 1 inch= 100 ft (Vertical Exaggeration x 2)

Line 10 Seismic Reflection and Refraction Profiles
Showing Interpretation of Subsurface Layering and Faulting
LADWP North Haiwee Dam
Inyo County, California



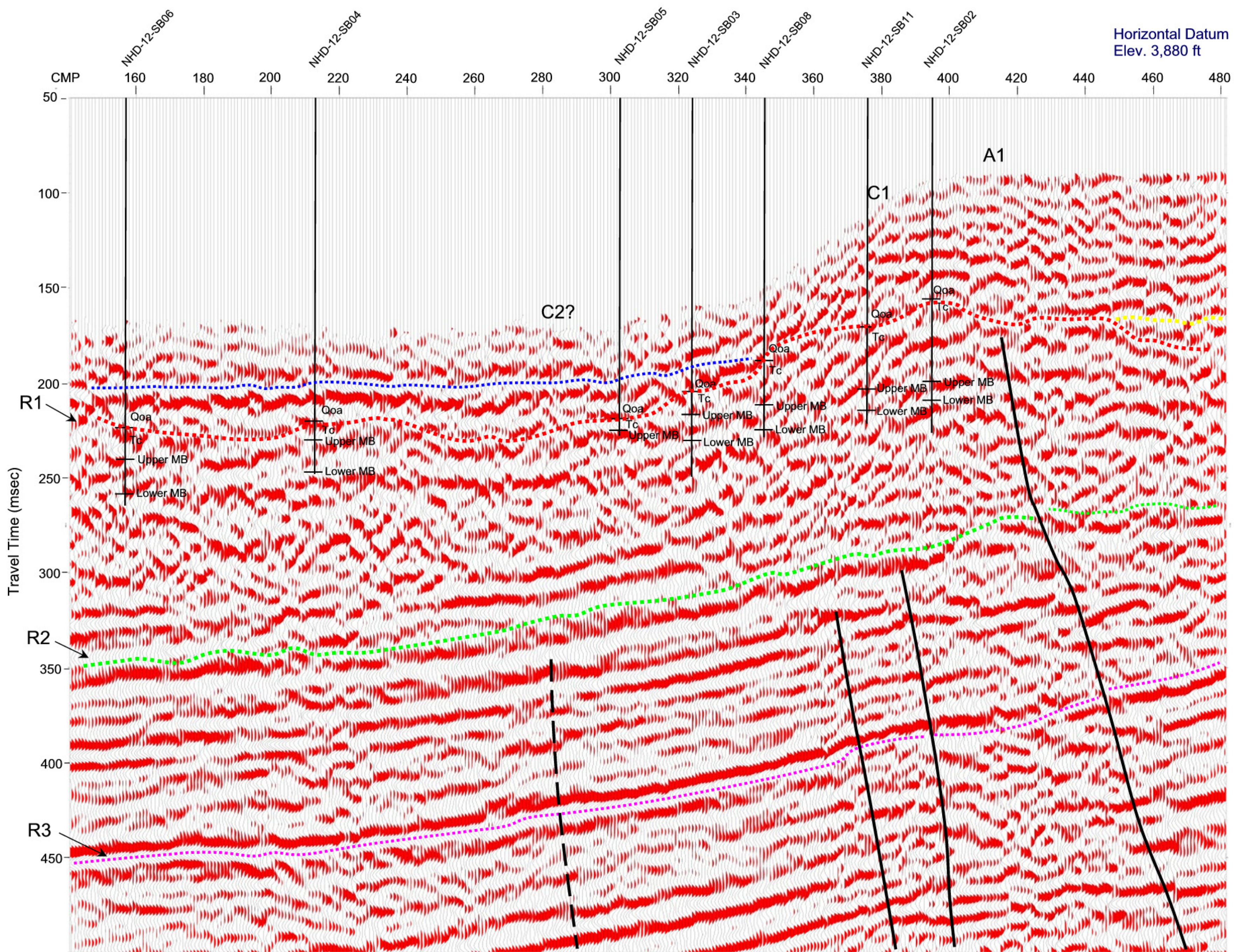
Profiles Shown at Approximate Same Horizontal Positioning
 Horizontal Scale 1 inch= 100 ft
 Vertical Scale Refraction 1 inch= 100 ft

Line 11 Seismic Reflection and Refraction Profiles
 Showing Interpretation of Subsurface Layering and Faulting
 LADWP North Haiwee Dam
 Inyo County, California

Line 9 Seismic Reflection Profile Showing Enlarged View of East Abutment Area with Sonic Borehole Lithologic Contacts

SW

NE



Horizontal Datum
Elev. 3,880 ft

Profile Horizontal Scale 1 inch= 100 ft

Shows Sonic Boreholes Along Line 9 Completed in 2012
Equivalent Seismic Wave Travel Time Positioning of
Lithologic Contacts Estimated Based on
Approximate Depth-to-Travel Time Conversion
Using Velocities From Refraction Tomography.

Interpretation of Seismic Reflection Patterns:

- Valley Alluvium Water Table
- Older Alluvial Surface
- Pliocene Coso Formation (Tc) Bedrock Surface (R1)
- Coso Formation Bedding (R2)
- Deeper, Conformable Tertiary Bedding (R3)

Line 9 Seismic Reflection Profile of East Abutment Area
Showing Correlation to Sonic Borehole Logs
LADWP North Haiwee Dam
Inyo County, California

Revised Interpretation 10/12

Figure 13
Advanced Geoscience, Inc.